J. Chem. Eng. Data **1996,** *41,* 987−1004

Reviews

Applications of Calorimetry to Nonelectrolyte Solutions

J. Bevan Ott*

Department of Chemistry and Biochemistry, Brigham Young University, Provo, Utah 84602

Jadwiga T. Sipowska

Department of Chemistry, University of Michigan−Flint, Flint, Michigan 48502

This paper describes the application of calorimetry to the measurement of the excess molar enthalpies H_m^E for binary mixtures of nonelectrolytes. Batch, displacement, and flow calorimeters are described, using as examples the batch calorimeter of McGlashan;, the displacement calorimeters of Van Ness and of Marsh and Stokes, and the flow calorimeters of Christensen, Wormald, and Picker. Applications are described using calorimeters to measure H_m^E for {(nonpolar + nonpolar), (polar + nonpolar), and (polar + polar)} mixtures. Excess enthalpies for liquid mixtures containing charge-transfer complexes and hydrogen bonds are used to help in understanding the nature of the molecular interactions in these systems. Applications involving measurements on liquid, gas, and supercritical fluid mixtures, including measurements in the near-critical region, are also described. The use of calorimetric measurements to determine {(liquid + liquid) and (vapor + liquid)} phase equilibria is discussed. Finally, equations used to represent $H_m^E(x)$ measurements are summarized.

1. Introduction

The earliest attempts at measuring the heat effects when nonelectrolytes are mixed date back to the beginnings of the century when workers such as Clarke (05-cla), Bose (07-bos), and Baud (15-bau) reported heats of mixing for mixtures such as alcohols with water, hydrocarbons with halogenated hydrocarbons, and aromatic with aliphatic hydrocarbons. Hildebrand (17-key/hil) became involved in the measurement of heats of mixing as early as 1917 in his study of the solubilities {(liquid + liquid) equilibria} in the (aniline + hexane) system.

Heats of mixing are now referred to as excess molar enthalpies H_m^E, as defined in section 2. Excess molar enthalpies can be obtained from calorimetric measurements or the temperature effect on the excess molar Gibbs energy G_m^E {usually obtained from (vapor + liquid) phase equilibrium measurements} using eq 13. However, obtaining temperature derivatives of G_m^E as required by eq 13 of the accuracy necessary to give reliable H_m^E is very difficult to do, and this method is not often used to obtain H_m^E. (The usefulness of eq 13 usually involves the reverse process. That is, H_m^E values obtained calorimetrically are used to calculate the effect of temperature on G_m^E.) Thus, there are no good alternatives to the calorimeter for measurement of excess molar enthalpies, and the calorimeters used by the early investigators were very crude. Clarke (05-cla) used a Bunsen ice calorimeter, which restricted his work to 0 °C. For the others, mixing was usually accomplished in a Dewar flask and the temperature change measured with a Beckman thermometer or equivalent.

The work of Hirobe (25-hir), published in 1925, deserves special recognition. He developed a more sophisticated isothermal calorimeter and used it to measure the excess molar enthalpies for 51 binary mixtures. His results, some of which were obtained as early as 1910, are often within a few percent of results obtained with the best modern calorimeters.

It is not correct to draw the conclusion as a result of the success of Hirobe that it is easy to make accurate measurements of excess molar enthalpies for mixtures of nonelectrolytes. The literature is full of results which are suspect. It was not until the development of modern calorimeters in the past 30 years that reliable results have been obtained. Even now, incorrect results find their way into the literature when care is not taken to ensure accurate measurements.

The mixing process can be endothermic or exothermic, with the amount of heat usually small. Problems such as incomplete mixing, inaccurate temperature measurement, and unknown heat leaks can cause serious errors. A potentially serious source of error involves the heat effects caused by evaporation or condensation of vapor from or into the liquid phase during mixing, if a vapor phase is present in the calorimeter and the components are volatile. Modern calorimeters used to measure excess molar enthalpies are designed to ensure complete mixing, provide the necessary temperature measurement and control, and eliminate the vapor phase, to minimize these sources of error.

2. Excess Molar Thermodynamic Functions

An excess molar function Y_m^E is the difference between the change $\Delta_{mix}Y$ for the molar thermodynamic function Y_m on forming one mole of mixture and that of forming one mole of ideal mixture, that is, for the process

$$x_1A + x_2B + ... = \text{mixture} \tag{1}$$

$$Y_m^E = \Delta_{mix}Y_m - \Delta_{mix}Y_m^{id} \tag{2}$$

S0021-9568(96)00105-7 CCC: $12.00

where x_1, x_2, ... are the mole fractions of components A, B, ... and Y_m is the molar thermodynamic function: enthalpy (H_m), Gibbs energy (G_m), entropy (S_m), volume (V_m), or heat capacity ($C_{p,m}$). Y_m^{id} is the molar thermodynamic function in an ideal mixture.

The ideal enthalpy, volume, and heat capacity of mixing are zero so that

$$H_m^E = \Delta_{mix}H_m \tag{3}$$

$$V_m^E = \Delta_{mix}V_m \tag{4}$$

$$C_{p,m}^E = \Delta_{mix}C_{p,m} \tag{5}$$

For Gibbs energy and entropy

$$\Delta_{mix}G_m^{id} = RT\sum x_i \ln x_i \tag{6}$$

$$\Delta_{mix}S_m^{id} = -R\sum x_i \ln x_i \tag{7}$$

so that

$$G_m^E = \Delta_{mix}G_m - RT\sum x_i \ln x_i \tag{8}$$

$$S_m^E = \Delta_{mix}S_m + R\sum x_i \ln x_i \tag{9}$$

The excess molar functions are related through the equation

$$G_m^E = H_m^E - TS_m^E \tag{10}$$

The excess molar Gibbs energy G_m^E is usually obtained from phase equilibria measurements and H_m^E from calorimetric measurements, with S_m^E then calculated from eq 10.

The pressure and temperature coefficients of H_m^E are calculated from eqs 11 and 12

$$(\partial H_m^E/\partial T)_p = C_{p,m}^E \tag{11}$$

$$(\partial H_m^E/\partial p)_T = V_m^E - T(\partial V_m^E/\partial T)_p \tag{12}$$

while H_m^E can be used to determine the effect of temperature on G_m^E through the relationship

$$\{\partial(G_m^E/T)/\partial T\}_p = -H_m^E/T^2 \tag{13}$$

Equations 11 and 12 are useful in correlating and understanding the calorimetric measurement of H_m^E, since they predict the effect of temperature and pressure. Equation 13 provides a method for predicting the effect of temperature on activity and hence, the activity coefficients.

3. Types of Calorimeters

Most H_m^E measurements are now made with one of three types of calorimeter: a batch calorimeter, a displacement calorimeter, or a flow calorimeter. All three are designed to eliminate the vapor phase, which can cause serious errors in the measurement.

a. Batch Calorimeter. In a batch calorimeter, the two components are loaded into separate compartments, then mixed, and the heat effect measured. An example of a batch temperature change calorimeter is described by Larkin and McGlashan (61-lar/mcg) and shown in Figure 1. The calorimeter consists of a glass vessel in which the upper half is separated into two compartments. The vessel is filled with mercury and immersed in a bowl of mercury.

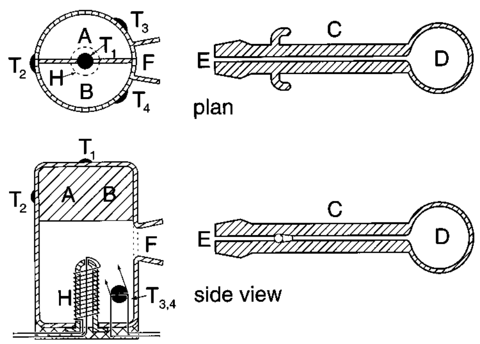

Figure 1. Batch calorimeter of Larkin and McGlashan (61-lar/mcg). A and B are the compartments which contain the fluids to be mixed. Movement of a column of mercury in the capillary C takes up the expansion or contraction upon mixing to prevent the formation of a vapor phase. Filling is accomplished through F, which can also be attached to the capillary through the tapered joint E. T_1, T_2, T_3, and T_4 are temperature thermistors. H is the calibration heater. Reprinted with permission from ref 61-lar/mcg. Copyright 1961 Royal Society of Chemistry.

The two components to be mixed are injected into the compartments A and B through opening F with a curved needle attached to a hypodermic syringe, which displaces the mercury from the compartments.

The capillary C is half-filled with mercury and attached to the vessel at F. The entire apparatus is then placed in a vacuum enclosure in a thermostat and equilibrated at the bath temperature. Rotation of the vessel through 180° mixes the components. The temperature change is measured with the four thermistors T_1, T_2, T_3, and T_4 placed at different positions on the surface or in the vessel. Electrical calibration is provided by the heater H. Changes in volume due to mixing are taken up by movement of the mercury in the capillary. This procedure prevents the appearance of a vapor phase.

Modifications of the Larkin–McGlashan calorimeter and other batch calorimeters have been used by a number of investigators. However, they have been largely replaced in recent years by the displacement calorimeter, and more recently, by flow calorimeters. The batch calorimeter has the disadvantage that the measurement at each composition requires refilling the calorimeter. Hence, the comparatively large number of independent measurements necessary to measure H_m^E over a range of compositions requires a considerable length of time.

b. Displacement Calorimeter. Displacement calorimeters have an advantage over batch calorimeters in that incremental additions of a second component can be made to the first component so that a series of H_m^E results over a range of composition can be made in one run. By reversing components, two runs can give a series of measurements that span the entire range of composition. Less chemical is required in a displacement calorimeter than for the batch calorimeter, and considerably less than for the flow calorimeter. The displacement calorimeter also allows for better control of heat leaks and can be designed to give results of high accuracy.

The power compensation displacement calorimeter as designed by Van Ness and colleagues (61-mra/van, 66-sav/win) is shown in Figure 2. The calorimeter mixing vessel is the Dewar flask A. One of the components to be mixed is weighed into this mixing vessel, all air is removed through a vent hole in piston B, and a plug is inserted into B to seal the vessel. The second component is stored in the feed bulb C. Small bore capillary tubing leads from C into A, with the open end in the mixing vessel submerged in mercury contained in the small cup E. Mixing is

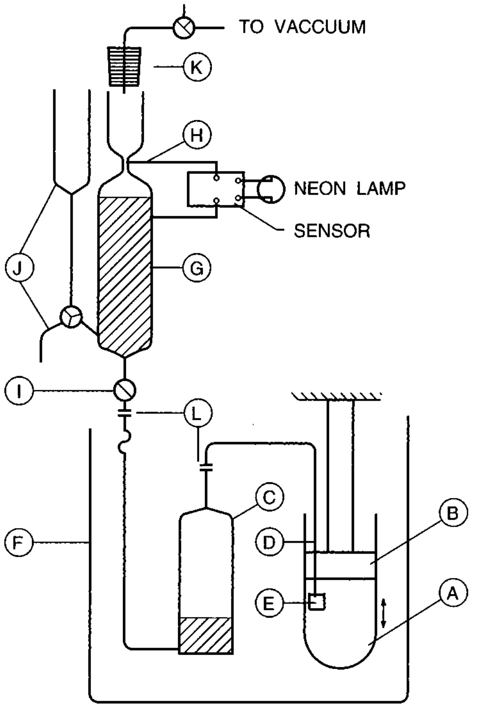

Figure 2. Van Ness displacement calorimeter (61-mra/van, 66-sav/win). The liquid in container C is added to the liquid in the Dewer flask A through line D and the mercury bubbler E. Movement of the piston B eliminates the vapor phase. Mercury in G displaces the fluid in C during mixing in A. Reprinted with permission from ref 66-sav/win.

accomplished by lowering the mixing vessel, which causes the second component to bubble through the mercury and into the flask. In the process, the piston B advances to increase the available volume in the flask. The head of mercury in G assures that a positive pressure will be applied to the mixing vessel during injection to prevent the formation of a vapor space in A. Mixing is aided by a stirrer in the mixing vessel.

With this design, the Van Ness calorimeter can only be used for endothermic mixing processes. In a typical run, energy is added with an electrical heater to keep the mixture isothermal as increments of the second component are added to the mixture, with the amount of electrical energy carefully measured during each addition. Each of these additions results in a value of H_m^E at a new and larger mole fraction. This process continues until over half of the mole fraction range is covered. Reversing the components covers the other half of the mole fraction range, with the result that H_m^E measurements are obtained at close mole fraction intervals over the entire range of composition. Temperature sensing is accomplished with a thermistor in a Wheatstone Bridge circuit.

In a later modification of the Van Ness calorimeter (66-win/van), a thermoelectric cooler was added, which allowed measurement of negative excess molar enthalpies.

Several other calorimeters based on the Van Ness design have been reported in the literature. An especially successful design is that developed by Marsh and co-workers (69-sto/mar, 70-ewi/mar-1), shown in Figure 3. In this apparatus, the calorimeter vessel is partially filled with mercury and partially with one of the components. The second component is then added in increments from a motor driven buret, which displaces the mercury. Electrical energy is added during the mixing process to keep the calorimeter at bath temperature (isothermal operation).

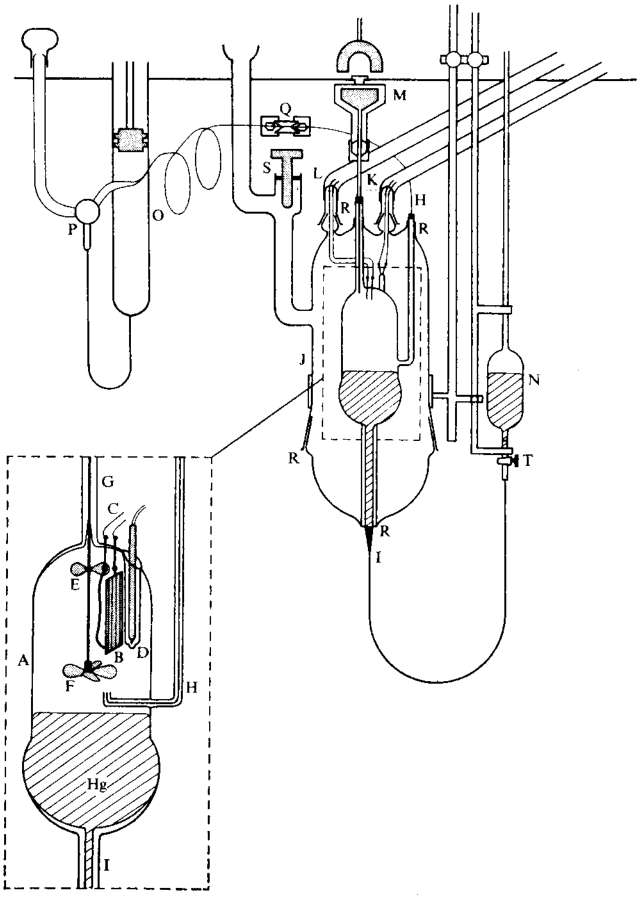

Figure 3. Displacement calorimeter of Marsh and Stokes (69-sto/mar, 70-ewi/mar-1). The calorimeter A is partly filled with one of the components. Mixing is accomplished by adding the second component through the capillary H, which displaces mercury from A. Heat is added electrically with the heater B, with the temperature monitored by the thermistor D to keep the calorimeter at constant temperature. E and F are stirrers while O is a motor driven buret. Reprinted with permission from ref 69-sto/mar. Copyright 1969 Academic Press.

As a result of the incremental addition, a single run measures H_m^E as a function of composition over slightly more than half of the composition range. Reversing the components in a second run completes the measurements over slightly more than the other half of the range of mole fractions. Overlap of the two sets of measurements in the middle is confirmation that the calorimeter has performed properly.

The original apparatus was restricted to endothermic processes, but in a later version (79-fre/ric, 80-mar/ott, 80-cos/hod), a Peltier cooler was added so that H_m^E could also be measured for exothermic processes. The displacement calorimeter of Marsh and co-workers is very reliable and has provided results of exceptionally high accuracy. However, the Van Ness and Marsh calorimeters both suffer from a limitation in that measurements are restricted to atmospheric pressure and to temperatures not too far removed from ambient. A strong interest in H_m^E results at high temperatures and high pressures, including measurements in the near-critical region and with supercritical fluids, requires a different concept. Flow calorimeters have been used very successfully to make these measurements.

c. Flow Calorimeter. Flow calorimeters have a major advantage over batch and displacement calorimeters in that measurements can be made over a wide range of pressure and temperature conditions. Thus, measurements can be made with gases as well as liquids. Flow calorimeters require large amounts of chemicals, which makes it difficult to measure H_m^E for rare and expensive

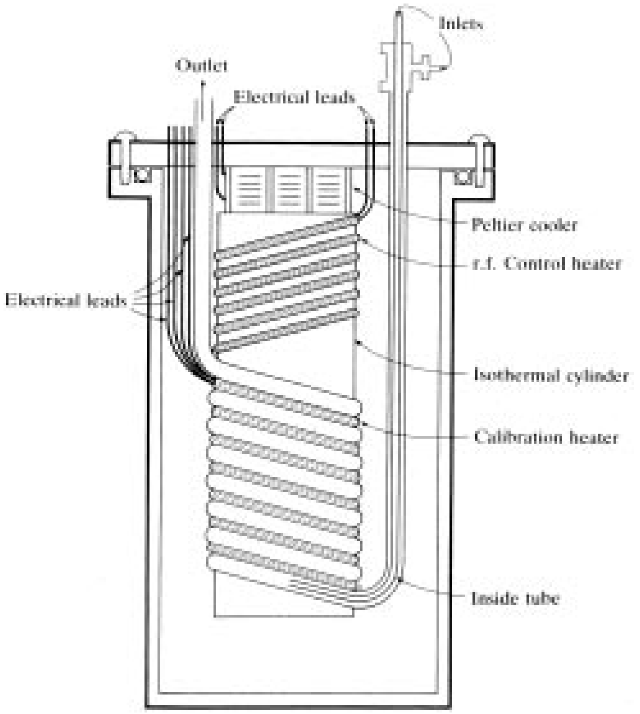

Figure 4. Christensen isothermal flow calorimeter (86-ott/sto). The operation of this calorimeter is described in the text.

substances, although measurements can often be made with corrosive and reactive chemicals that would not be compatible with batch or displacement calorimeters.

In an early version of a power compensated flow calorimeter designed by Christensen and co-workers (76-chr/han), fluids were mixed in a metal capillary tube wound on the surface of a flat metal plate. The plate was later replaced by a copper cylinder, as shown in Figure 4 (86-ott/sto). The metal capillary mixing coil is wound on the cylinder with a steel sheathed calibration heater wound between the turns of the coil. The top of the cylinder is in contact with a Peltier cooler, which is also in contact with a constant temperature bath surrounding the apparatus. Isothermal operation is obtained by balancing the cooling from the Peltier device with a pulsed heater. Values of H_m^E are obtained from changes in the frequency of the pulsed heater before and during mixing. This apparatus can be used to measure H_m^E for both endothermic and exothermic processes at pressures from (0.4 to 20) MPa and temperatures from (250 to 475) K (the high-temperature limit for the Peltier device). A modification by Christensen (84-chr/iza), which replaces the Peltier device with a controlled heat leak path, extends the temperature range to 673 K.

Wormald and colleagues (76-ell/wor, 77-wor/lew) have reported power-compensated flow calorimeters of a different design, which again can be used at high temperatures and pressures. The design used to measure H_m^E in liquid mixtures (76-ell/wor) is shown in Figure 5. The liquid components are brought together through tubes T_1 and T_2 and mixed at M over a heater wire H positioned in the center of the calorimeter. Complete mixing is accomplished with three reversals of flow of the liquids between concentric cylinders separated by a stainless steel gauze.

For endothermic processes, electrical heat is added to the central heater to ensure isothermal operation, with temperatures measured with a thermopile. For exothermic processes, two calorimeters are used. The temperature rise which occurs in the mixing vessel is matched by adjusting the electrical power supplied to the second calorimeter.

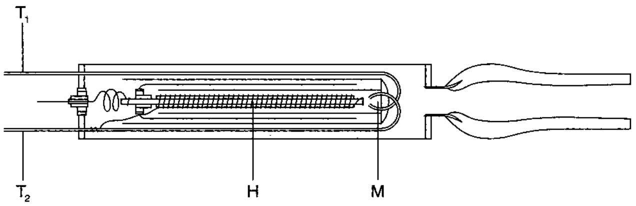

Figure 5. Wormald flow calorimeter (76-ell/wor) used to measure excess molar enthalpies for liquid mixtures. The operation of the calorimeter is described in the text. Reprinted with permission from ref 76-ell/wor. Copyright 1976 Royal Society of Chemistry.

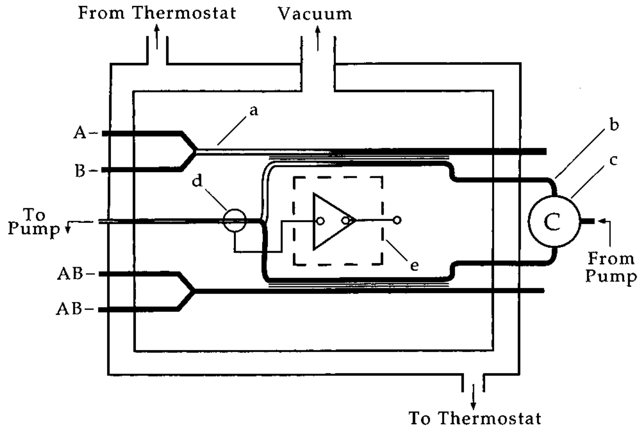

Figure 6. Flow calorimeter designed by Picker et al (74-pic). The operation of the calorimeter is described in the text. Reprinted with permission from ref 74-pic. Copyright 1974 Maclean Hunter.

The flow calorimeter of Picker (74-pic) shown schematically in Figure 6 is limited to near-ambient conditions but has been used for a number of years by different investigators. Fluids A and B flow into the calorimeter from a pump that is designed so that the ratio of the flow rates of the two liquids can easily be adjusted to change the composition of the mixture. The liquids are equilibrated to the temperature of the thermostat and mixed in tube a where a temperature change due to mixing occurs. The resulting AB mixture is brought back to the temperature of the thermostat as it flows down tube a by a countercurrent heat exchanger. In the process, the temperature of the heat-exchanger fluid changes. The AB mixture that is now at the temperature of the thermostat flows past a second heat exchanger. No heat is exchanged, since the mixture and heat-exchanger fluid are at the same temperature. The result is a heat-exchange fluid at a temperature corresponding to an excess enthalpy of zero that can serve to establish the baseline of the instrument. Fluid from the same source flows through both heat exchangers, with a modulating device c alternating fluid between the two. The detector d measures the temperature difference between the two sources of the fluid as they exit the heat exchangers. The output signal from the detector is amplified in e and serves as a measure of the excess enthalpy. An electrical heater attached to line a near the point of mixing serves to calibrate the calorimeter.

The Christensen and Picker calorimeters have been manufactured and sold commercially. Other commercial calorimeters have also been adapted and used to measure H_m^E. For example, Busey and co-workers (84-bus/hol) have inserted a coiled (platinum + rhodium) tube into a high-temperature Calvet calorimeter and used it to measure H_m^E at temperatures to 700 K and pressures to 50 MPa.

4. Applications with Liquid Mixtures

Excess enthalpies have been measured for many systems using a variety of calorimeters. J. J. Christensen and co-workers (82-chr/han) compiled a comprehensive handbook in 1982 which summarized the data reported in the literature to that date. Most of the measurements reported were made under near-ambient conditions, since calorimeters were not available before that time to extend H_m^E measurements to high temperatures and high pressures.

In 1984, C. Christensen and co-workers (84-chr/gme) made a similar compilation. In 1988 J. J. Christensen and colleagues (88-chr/row) published a supplementary volume, which contains a larger proportion of measurements obtained by flow calorimetry at extended pressures and temperatures.

If the temperature is well below the critical temperature of either component, the enthalpy of mixing of binary liquid mixtures is a good indication of the strength of the interactions between the molecules of the two different fluids as compared to the strengths of the interactions between the molecules in the two pure unmixed components. In general, strong interactions between unlike molecules in comparison to the strength of the interactions between the like molecules, give rise to negative enthalpies of mixing, whereas positive enthalpies of mixing indicate relatively weaker interactions between the unlike molecules.

The particular size and shape of the $H_m^E(x)$ curves depend on the nature of the forces existing in the mixtures, and these forces depend on the nature of the pure components being mixed together. Examples of binary mixtures taken from the literature illustrate the effect of polarity, shape, and size on H_m^E.

a. (Nonpolar + Nonpolar) Mixtures. Hydrocarbon mixtures are among the best examples of (nonpolar + nonpolar) mixtures. The excess enthalpies are usually relatively small and greater than zero and do not change significantly with temperature, so that the excess heat capacities are small. Unusual behavior does occur, and these special systems are interesting for theoretical interpretation.

Figure 7 gives $H_m^E(x)$ for $\{xn\text{-}C_6H_{14} + (1 - x)n\text{-}C_{10}H_{22}\}$, a typical (*n*-alkane + *n*-alkane) mixture (80-mar/ott). Also shown is G_m^E (obtained from vapor pressure measurements) and TS_m^E calculated from eq 10. Of interest is the fact that TS_m^E is larger than H_m^E, which results in a negative G_m^E. The excess molar volumes are also negative for this and similar systems. Thus, the molecules pack together upon mixing to decrease the volume, but increased disorder occurs, resulting in a larger entropy than in the ideal mixture.

A similar comparison is made in Figure 8 for $\{xc\text{-}C_6H_{12} + (1 - x)n\text{-}C_6H_{14}\}$ (69-mar/sto, 80-ott/mar). The excess molar enthalpy in this system is larger than in the previous example, and G_m^E is greater than zero. The excess molar entropy expressed as TS_m^E is smaller than H_m^E, although still much larger than in the (hexane + decane) system. For this system, V_m^E is greater than zero (80-ott/mar). This, along with the large S_m^E, indicates the destruction of structure resulting from mixing the chainlike *n*-alkane with the globular cycloalkane.

Marsh and co-workers have measured H_m^E for the various binary combinations of the C_5 through C_8 cycloalkanes (69-sto/mar-1, 70-ewi/lev, 74-ewi/mar, 70-ewi/mar, 74-ewi/mar-1). The results at 298.15 K are shown in Figure 9 and illustrate the unexpected diversity that can occur. All of the H_m^E results are small, but the (cyclopentane + cyclooctane) (69-sto/mar-1, 70-ewi/lev) and (cyclopentane + cyclohexane) (74-ewi/mar, 70-ewi/mar) systems have much larger excess molar enthalpies than the others, with H_m^E negative in the former and positive in the latter. On the other hand, H_m^E for the (cyclopentane + cycloheptane) (74-ewi/mar) system is small and s-shaped, with H_m^E changing

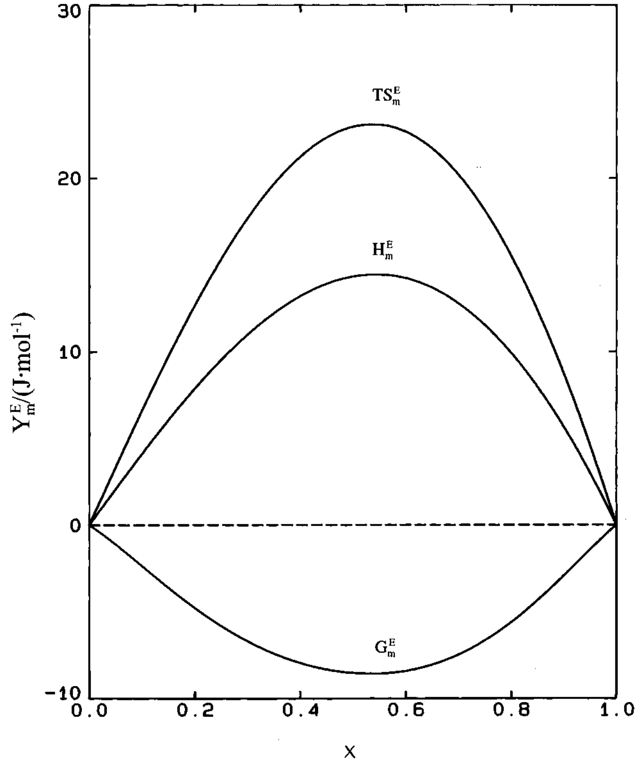

Figure 7. Comparison of H_m^E, G_m^E, and TS_m^E at 298.15 K for $\{xn\text{-}C_6H_{14} + (1 - x)n\text{-}C_{10}H_{22}\}$ (80-mar/ott).

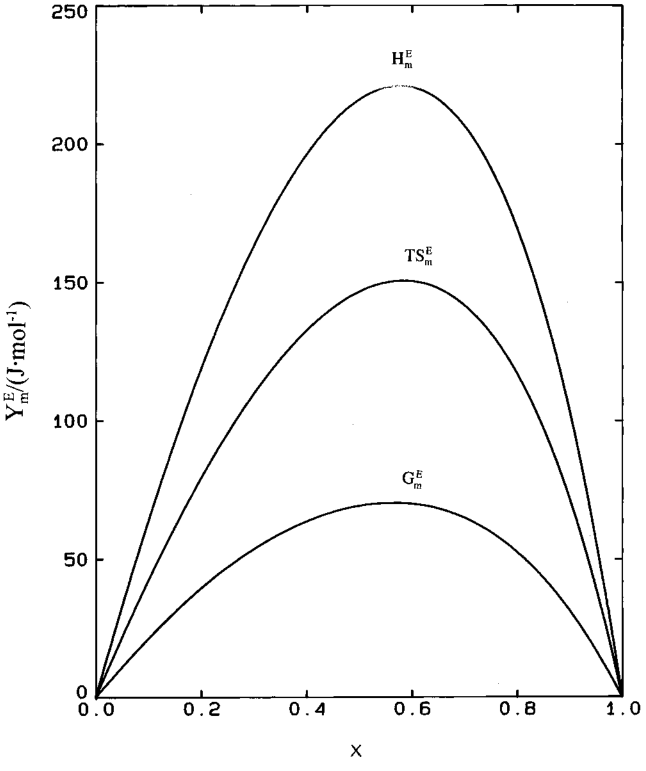

Figure 8. Comparison of H_m^E, G_m^E, and TS_m^E at 298.15 K for $\{xc\text{-}C_6H_{12} + (1 - x)n\text{-}C_6H_{14}\}$ (69-mar/sto, 80-ott/mar).

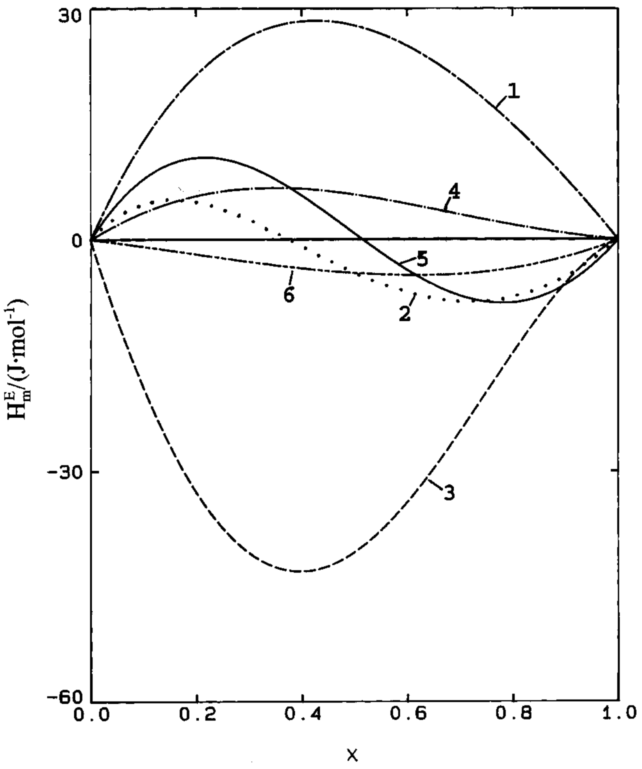

Figure 9. Comparison of H^E_m at 298.15 K for {xc-C_mH_{2m} + (1 − x)c-C_nH_{2n}} with m less then n. The values of m and n are as follows: (1) m = 5, n = 6; (2) m = 5, n = 7; (3) m = 5, n = 8; (4) m = 6, n = 7; (5) m = 6, n = 8; (6) m = 7, n = 8.

from positive to negative with increasing mole fraction of pentane.

For the (cyclohexane + cycloheptane) (74-ewi/mar-1), system, H^E_m is positive, with the maximum shifted toward the low mole fraction of the smaller cycloalkane. For (cycloheptane + cyclooctane) (74-ewi/mar-1) H^E_m is positive with the maximum shifted toward the high mole fraction of the smaller alkane. For (cyclohexane + cyclooctane) (74-ewi/mar), an s-shaped $H^E_m(x)$ curve is obtained.

Ewing and Marsh (77-ewi/mar) have suggested that the unusual properties in the cyclopentane systems are due to the lack of flexibility (hindered conformational changes) of the C_5 ring, but these systems need to be understood better before all of the effects can be adequately explained. They illustrate how little we understand about the nature of the effects which contribute to the H^E_m in hydrocarbon mixtures.

The (cyclohexane + n-hexane) system has been thoroughly investigated by a number of laboratories and H^E_m is well established for this system so that it is often used as a test system to verify the operation of new calorimeters. The equation (78-mar) {modified here to express H^E_m in terms of (1 − 2x) instead of x} that is used to calculate H^E_m at 298.15 K for {xc-C_6H_{12} + (1 − x)n-C_6H_{14}}is

$$H^E_m/\text{J·mol}^{-1} = x(1-x)\{866.10 - 249.4(1-2x) + 97.0(1-2x)^2 - 31.8(1-2x)^3\} \quad (14)$$

The excess molar enthalpy for (cyclohexane + n-hexane) is small. The (benzene + cyclohexane) system (69-sto/mar) is often used instead as a test system when a larger H^E_m is needed. The equation used for test purposes, for {xc-C_6H_{12} + (1 − x)C_6H_6} at 298.15 K is

$$H^E_m/\text{J·mol}^{-1} = x(1-x)\{3197.3 + 160.3(1-2x) + 121.4(1-2x)^2 + 39.2(1-2x)^3\} \quad (15)$$

b. (Polar + Nonpolar) Mixtures. Mixtures of a liquid containing nonpolar molecules (such as an alkane) with a liquid consisting of polar molecules (such as a halogenated alkane, nitrile, ether, or ketone) usually have a positive H^E_m, the value of which depends on the polarity of the polar compound and the size and shape of the molecules of both components.

Haloalkanes are moderately polar. The excess molar enthalpy obtained when they are mixed with alkanes has been considered to result from two major contributions (80-val/lop): intermolecular interactions, and the energy effect associated with changes in molecular orientation upon mixing, referred to as the CMO (the correlation of molecular orientation) effect. The contribution of CMO to H^E_m depends not only on the correlation degree but also on the ability of the other component to act as an order-breaker.

Figure 10 summarizes the trends in H^E_m observed for (alkane + haloalkane) mixtures. The equimolar excess molar enthalpy (x = 0.5) increases with an increase of alkane size due to the CMO effect and to the dilution effect, since both intensify with an increasing molar mass of the alkane. An increase in the size of the haloalkane molecule has an opposite effect on H^E_m since the polarity of these molecules decreases as their size increases.

By comparing the H^E_m obtained for branched and linear haloalkanes, it becomes evident that globular molecules are better order-breakers than are linear ones.

As the polarity of the polar compound increases, (liquid + liquid) phase separation may occur, as is the case for nitroalkanes and alkylnitriles mixed with alkanes. The $H^E_m(x)$ curves contain a linear region in the concentration range corresponding to the miscibility gap. Figure 11 compares H^E_m at 348.15 K and 15 MPa for {C_nH_{2n+2} + (1 − x)CH_3CN} (89-ott/nee, 91-ott/sip, 92-woo/sip) with n = 2−4 and (xc-C_6H_{12} + (1 − x)CH_3CN) (88-ott/pur). Again, H^E_m increases with increasing molar mass of the alkane. Solubility decreases with increasing molar mass of the alkane, with (liquid + liquid) phase separation occurring in the (cyclohexane + acetonitrile) system. {Phase separation also occurs in the (ethane + acetonitrile) system, which is related to the fact that the ethane is a supercritical fluid at 348.15 K.}

c. (Polar + Polar) Mixtures. The sign and magnitude of H^E_m for (polar + polar) mixtures depends upon the relative strengths of the interactions between the like molecules which are present in the pure liquids and the interactions between unlike molecules which result from the mixing process. Excluding systems containing hydrogen bonds which will be described later, H^E_m is often greater than zero and nearly symmetrical with mole fraction for (polar + polar) systems, and if the molecules of both components have similar dipole moments, H^E_m is small in magnitude. For example, $H^E_m(x = 0.5)$ is 20 J·mol^{-1} at 297.48 K for (chlorobenzene + bromobenzene) (55-can/che) and zero at 318.15 K (within the accuracy of the measurements) for (acetonitrile + nitromethane) (56-bro/foc).

In other examples, larger values of $H^E_m(x = 0.5)$ are obtained. For (2-propanone + diethyl ether) (58-dri/kiv) and (2-propanone + dimethyl sulfoxide) (71-cle/pig) the values at 298.15 K are 565 J·mol^{-1} and 335 J·mol^{-1}, respectively. There are exceptions to the positive H^E_m.

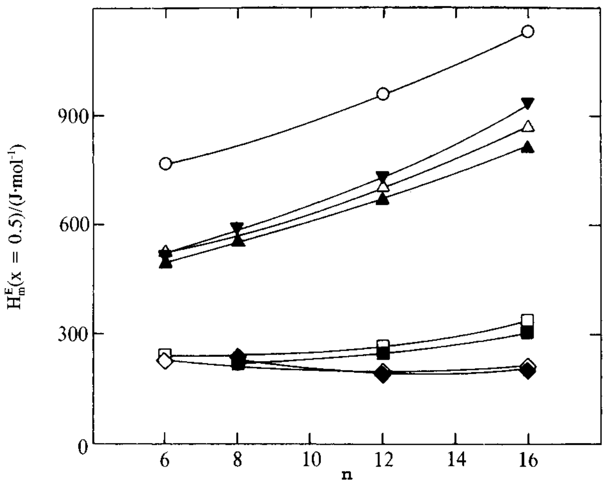

Figure 10. Trends in $H^E_m(x = 0.5)$ observed for (alkane + haloalkane) mixtures. n refers to the number of carbon atoms in the n-alkane C_nH_{2n+2}. The symbols distinguish the various haloalkanes as follows: (○), CH_3CH_2Br; (▼), $(CH_3)_3CBr$; (△), $CH_3(CH_2)_3Br$; (▲), $CH_3(CH_2)_3Cl$; (□), $CH_3(CH_2)_{11}Br$; (■), $CH_3(CH_2)_{11}Cl$; (◇), $CH_3(CH_2)_{15}Br$; (◆), $CH_3(CH_2)_{15}Cl$. Reprinted with permission from ref 80-val/lop. Copyright 1980 Academic Press.

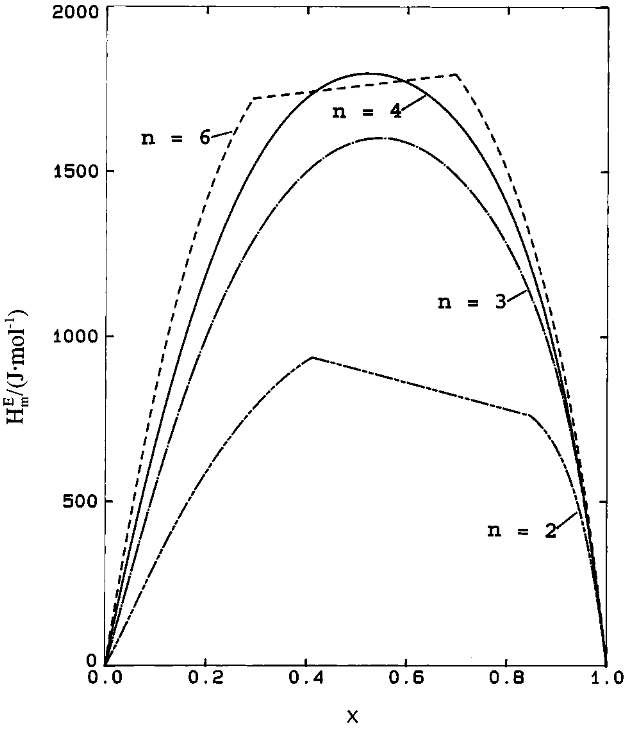

Figure 11. Comparison of excess molar enthalpies at $T = 348.15$ K and $p = 15$ MPa for $\{xC_nH_{2n+2} + (1 - x)CH_3CN\}$ (89-ott/nee, 91-ott/sip, 92-woo/sip) with $n = 2–4$, and for $\{xc\text{-}C_nH_{2n} + (1 - x)CH_3CN\}$ (88-ott/pur) with $n = 6$. The $H^E_m(x)$ curves become more positive with increasing n. The linear regions of the curves for $n = 2$ and $n = 6$ result from phase separation. At 348.15 K, C_2H_6 is a supercritical fluid while all other components are liquids. Reprinted with permission from ref 92-woo/sip. Copyright 1992 Academic Press.

For example, H^E_m $(x = 0.5) = -108$ J·mol^{-1} at 298.15 K for (2-propanone + acetonitrile) (81-nag/tam).

Letcher and Domańska (94-let/dom) have reported H^E_m at 298.15 K for mixtures of acetonitrile with a series of ethers. The values obtained vary from a positive $H^E_m(x)$ with a maximum of 1260 J·mol^{-1} for (acetonitrile + di-n-butyl ether), to an s-shaped $H^E_m(x)$ for (acetonitrile + 1,4-dioxane), with a maximum of 34 J·mol^{-1} at a low mole fraction of acetonitrile to a minimum of -28 J·mol^{-1} at a high mole fraction.

These results illustrate the effect of the relative strength of the like and unlike interactions on the magnitude of H^E_m. A major contribution to the large positive H^E_m in the (acetonitrile + di-n-butyl ether) system is the energy required to overcome the attractions between the highly polar acetonitrile molecules as they are diluted and separated by the alkyl groups of the di-n-butyl ether. In the (acetonitrile + 1,4-dioxane) system, attractions between sites on like molecules are replaced by attractions of similar strength between sites on unlike molecules (even though 1,4-dioxane is nonpolar) and H^E_m is small.

d. Mixtures Containing Charge Transfer Complexes. Specific interactions can occur in solution which can have a significant effect on H^E_m. An example is the formation of charge-transfer (or donor–acceptor) complexes. Both polar and nonpolar molecules can form these complexes. For example, solid (tetrachloromethane + aromatic) molecular addition compounds have been identified (62-ott/goa). The interractions that result in the formation of solid compounds in these mixtures of nonpolar molecules have been attributed to a charge-transfer process in which electrons from the π ring of the aromatic molecule are transferred to the empty 3d orbitals of the chlorines in the tetrachloromethane (96-ott/goa). It is expected that an equilibrium process in the liquid mixture would result in the formation of similar liquid-phase charge-transfer complexes, even though an absorption band in the UV–visible part of the spectrum due to the charge-transfer process has not been observed. {Slifkin (71-sli) describes the procedures to follow in identifying charge-transfer complexes in solution. He notes that the absorption band may be difficult to observe since it can fall in the far ultraviolet region of the spectrum or the extinction coefficient ϵ and/or the equilibrium constant K_c may be small so that the product $K_c\epsilon$, which gives the extent of absorption, is small.}

The size of H^E_m for mixtures that form charge-transfer complexes depends upon the strength of the charge-transfer bond. This bond is weak in (benzene + tetrachloromethane) and a small H^E_m of (98, 112, and 124) J·mol^{-1} is obtained at (288.15, 298.15, and 308.15) K, respectively (66-vil/sta). In general, the temperature coefficient of H^E_m is positive for systems involving charge transfer since the equilibrium resulting in the formation of the charge-transfer complex is less favorable at higher temperatures.

The positive excess molar enthalpy decreases and can become negative as the strength of the charge-transfer complex increases. For example, H^E_m for (1,4-dimethylbenzene + tetrachloromethane) (67-ras/nat) is (-28, -21, and -15) J·mol^{-1} at the same three temperatures as above. The charge-transfer complex in this system is stronger than in (benzene + tetrachloromethane) because of the higher electron density on the aromatic ring in 1,4-dimethylbenzene. Even more extreme examples are the (N,N-dimethylformamide + tetrachloromethane) (66-qui) and (1,4-dioxane + tetrachloromethane) (80-cos/hod) systems, where $H^E_m = -354$ J·mol^{-1} and -252 J·mol^{-1}, respectively, at 298.15 K. It has been suggested that the electron pair on the nitrogen in N,N-dimethylformamide and the electron pair on the oxygen in 1,4-dioxane make these molecules moderately strong electron donors, and relatively strong charge-transfer complexes form with tetrachloromethane (96-ott/goa).

e. Mixtures Containing Hydrogen Bonds. The excess molar enthalpies in mixtures in which one or both components form hydrogen bonds have long been of special interest in calorimetry. In (alkanol + alkane) systems, association occurs between the alkanol molecules as a result of hydrogen bonding. The excess molar enthalpy that results when an alkanol and alkane are mixed is usually considered as resulting from two different effects, a chemical part due to the breaking of hydrogen bonds and a physical part due to the interactions between the species present in the solution, with the chemical part usually dominating.

The excess molar enthalpies for (alkanol + alkane) mixtures are positive and asymmetrical, with the maximum value occurring at a low mole fraction of the alkanol. The excess molar enthalpy increases with increasing temperature up to approximately the boiling point of the alkanol, where the temperature coefficient may become negative. Thus, if one goes to a high enough temperature, H_m^E should first increase, then go through a maximum, and then decrease. Values of H_m^E are strongly dependent on the size and shape of the alkanol molecules. For alkan-1-ols H_m^E increases as the molar mass of the alkanol increases. The effect of the shape of the alkanol molecules is illustrated by the excess molar enthalpy results for hexane with four isomeric butanols (69-bro/foc) where the values of H_m^E decrease in the order (hexane + 2-methyl-propan-2-ol) > (hexane + butan-2-ol) > (hexane + 2-methyl-propan-1-ol) > (hexane + butan-1-ol).

The excess molar entropies for (*n*-alkanol + *n*-alkane) systems increase with the number of carbon atoms in the alkanol and, in general, are negative at high mole fractions of alkanol where translational and orientational restrictions are high but become positive at lower mole fractions where a larger number of hydrogen bonds are broken. The excess molar enthalpies and entropies are thus both asymmetric functions of mole fraction, with the resultant G_m^E more symmetrical and decreasing as the size of the alkanol increases.

Bellemans (76-bel) and Wóycicka (79-wóy) applied specific association models to H_m^E/x_Ax_B curves for dilute solutions of alkanols in alkanes and concluded that for most of the alkanols, cyclic trimers and cyclic pentamers, along with straight-chain polymers, are formed. The values of the association constants were calculated. Stokes (77-sto) made a similar analysis of H_m^E and spectroscopic results for (ethanol + cyclohexane) mixtures, in which he calculated the energy of the hydrogen bond and the association constants for straight-chain and cyclic complexes.

The excess molar enthalpies for (alkan-1-ol + benzene) mixtures are much more positive than those for the (alkan-1-ol + *n*-hexane) mixtures. According to Barker (52-bar), more alkanol hydrogen bonds are broken in benzene solutions than in hexane solutions due to the stronger interaction between benzene and the hydroxyl hydrogen.

Ott and co-workers (96-ott/bro) have recently completed an extensive study of H_m^E for all the binary mixtures of ethane, propane, or butane with methanol, ethanol, propan-1-ol, or butan-l-ol. The study correlated the effect of size, shape, temperature, and pressure on H_m^E for these simple (alkane + alkanol) mixtures. Of special interest is the effect on H_m^E as the critical temperature of the alkane is approached and exceeded for the systems containing ethane. When this happens, large H_m^E are obtained that are very pressure as well as temperature dependent.

Another interesting group of mixtures are those in which one of the components contains hydrogen bonds while the second does not, and hydrogen bonds can also occur between molecules of the two components. Examples are (2-propanone + alkanol) (71-ben/mur, 27-par/caf, 72-cam/ana, 74-kiy/ana) mixtures, in which excess molar enthalpies are positive and nearly symmetrical about $x = 0.5$. Dilution of the alkanol breaks hydrogen bonds between the alkanol molecules and leads to absorption of energy. Dilution of 2-propanone reduces the (dipole + dipole) interactions between the 2-propanone molecules, leading also to absorption of energy. However, 2-propanone molecules contain the carbonyl group, which can hydrogen bond to the hydroxyl hydrogen of the alkanol. The formation of these hydrogen bonds produces a compensating negative energy effect. Positive S_m^E values suggest that the orientational disorder accompanying the breakup of both the 2-propanone structure and the alkanol hydrogen bonds are the main contributions to the positive H_m^E and S_m^E.

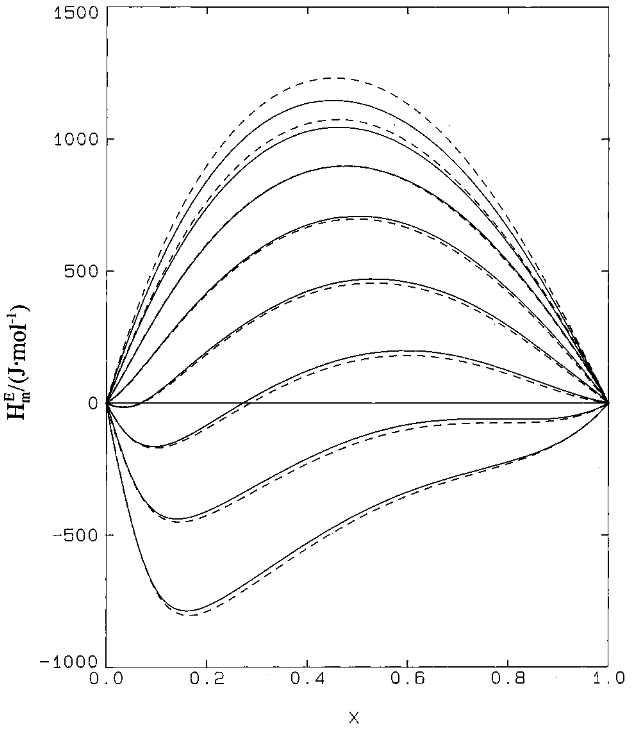

Figure 12. Excess molar enthalpies for $\{xC_2H_5OH + (1 - x)H_2O\}$ (87-ott/sto) at 298.15, 323.15, 348.15, 373.15, 423.15, 448.15, and 473.15 K. The solid lines give H_m^E at a pressure of 5 MPa, while the broken lines are for H_m^E at 15 MPa. H_m^E increases with increasing temperature so that the bottom curves are at 298.15 K and the top curves are at 473.15 K. Reprinted with permission from ref 87-ott/sto. Copyright 1987 Academic Press.

Another group of hydrogen bonded systems are those in which hydrogen bonds (of any appreciable strength) are not present in either pure component, but do form in the mixture. Probably the most studied examples involve mixing trichloromethane with a second component in which the molecules contain a fluorine, oxygen, or nitrogen atom, but no hydrogens which can form a hydrogen bond. (Trichloromethane + 2-propanone) is an example of such a system. A hydrogen bond forms between the two components when they are mixed, resulting from the interaction of the hydrogen in the trichloromethane (which has a high positive charge due to the combined inductive effect of the three chlorine atoms) with the carbonyl oxygen of the 2-propanone. In systems such as this, H_m^E is large in magnitude, but negative, due principally to the formation of the hydrogen bond. In (trichloromethane + 2-propanone) (75-han/fen), H_m^E at 298.15 K has a minimum value of -1.93 kJ·mol^{-1}.

(Ethanol + water) is an example of a system in which strong hydrogen bonds are present between both like and unlike molecules. Figure 12 shows $H_m^E(x)$ for this mixture

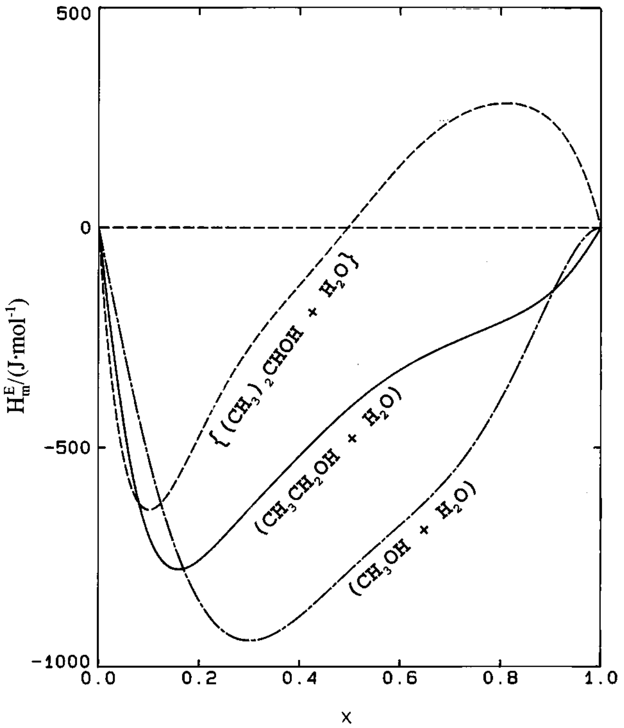

Figure 13. Comparison of the excess molar enthalpies at a temperature of 298.15 K and a pressure of 0.1 MPa for $\{x\mathrm{CH_3OH} + (1 - x)\mathrm{H_2O}\}$ (85-bat/row), $\{x\mathrm{CH_3CH_2OH} + (1 - x)\mathrm{H_2O}\}$ (80-cos/hod), and $\{x\mathrm{(CH_3)_2CHOH} + (1 - x)\mathrm{H_2O}\}$ (85-bat/row).

at eight temperatures and two pressures (87-ott/sto). The large negative $H^{\mathrm{E}}_{\mathrm{m}}$ at low temperatures with the minimum shifted toward the low mole fraction of alkanol, and with a large positive temperature coefficient, has been explained as resulting from formation of hydrogen-bonded (alkanol + water) complexes in which the alkyl group of the alkanol is situated in a cage of water molecules (90-ott). At high temperatures, few hydrogen bonds are present and positive excess molar enthalpies result. At intermediate temperatures, the $H^{\mathrm{E}}_{\mathrm{m}}$ results are also intermediate in value.

Methanol and other alkanols mixed with water show similar excess molar enthalpy results. Figure 13 compares $H^{\mathrm{E}}_{\mathrm{m}}$ at 298.15 K for methanol (85-bat/row), ethanol (80-cos/hod), and propan-2-ol (85-bat/row) mixed with water. The shift in the minimum to lower x with increasing molar mass of the alkanol can be explained as being due to the participation of more water molecules in the formation of the complex as the mass and, hence, the size of the alkanol increases. (An increased number of water molecules is necessary to form a larger cage to surround the larger alkyl group.)

(Ethanol + water) has been recommended as a reference system for testing mixing calorimeters (87-ott/sto), especially at high temperatures and pressures. The excess molar enthalpy as a function of composition at several temperatures and pressures can be represented by equations with the coefficients given by Ott and co-workers (86-ott/sto, 87-ott/sto).

An exchange of hydrogen bonds also occurs when alkanols are mixed with amines. These systems are interesting in that negative $H^{\mathrm{E}}_{\mathrm{m}}$ values that are very large in magnitude can be obtained. For example, the minimum $H^{\mathrm{E}}_{\mathrm{m}}$ for (methanol + dimethylamine) at $T = 298.15$ K is approximately -4.6 kJ·mol^{-1} (70-nak/tou). This $H^{\mathrm{E}}_{\mathrm{m}}$ is one of the most negative obtained for mixing liquids where the temperature is well below the critical temperatures of the components. Funke et al. (89-fun/wet) have suggested that the large $H^{\mathrm{E}}_{\mathrm{m}}$ in these systems is a result of a strong hydrogen bond that forms between alkanols and amines, which can exceed -40 kJ·mol^{-1}, while hydrogen bonds between alkanols and between amines are approximately -25 kJ·mol^{-1} and -10 kJ·mol^{-1}, respectively.

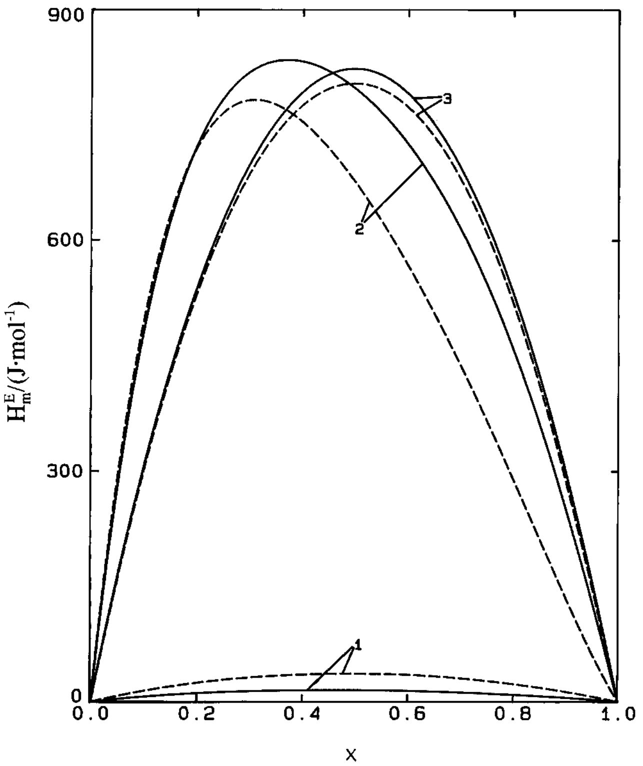

Figure 14. Comparison of the pressure effect on $H^{\mathrm{E}}_{\mathrm{m}}$ at ambient temperature. The examples of different types of liquid mixtures are (1) $\{xn\text{-}\mathrm{C_6H_{14}} + (1 - x)n\text{-}\mathrm{C_{10}H_{22}}\}$ (80-hei/lic) at 0.1 and 48.5 MPa, (2) $\{x\mathrm{(CH_3)_2CHOH} + (1 - x)n\text{-}\mathrm{C_7H_{16}}\}$ (81-hei) at 0.1 and 55.5 MPa, and (3) $\{xn\text{-}\mathrm{C_4H_{10}} + (1 - x)\mathrm{CH_3Cl}\}$ (92-gru/sip) at 5 and 15 MPa. The solid lines represent the lower pressure, and the broken lines represent the higher pressure.

5. Applications Involving Measurements at Temperature and Pressure Extremes

a. Liquid Mixtures. Excess molar properties of liquid mixtures at high pressures and at high temperatures are of importance in thermodynamics. As Heintz and Lichtenthaler (80-hei/lic) have pointed out, the high-pressure thermodynamic behavior of fluids and their mixtures is very sensitive to the nature of the intermolecular interactions, and therefore, data of excess molar properties at high pressures provide an important test of modern fluid theories. Heintz and Lichtenthaler were among the first to perform systematic measurements of $H^{\mathrm{E}}_{\mathrm{m}}$ for liquid mixtures at high pressures.

Liquids at temperatures well below their critical temperatures have small compressibilities. Pressure causes only small changes in the intermolecular interactions, and usually only a weak dependence of $H^{\mathrm{E}}_{\mathrm{m}}$ on pressure is observed under these conditions. Figure 14 shows the pressure dependence of $H^{\mathrm{E}}_{\mathrm{m}}$ for different types of mixtures (80-hei/lic, 81-hei, 92-gru/sip). Hydrocarbon mixtures have a positive $(\partial H^{\mathrm{E}}_{\mathrm{m}}/\partial p)_T$, while for mixtures of (polar + nonpolar) compounds, $(\partial H^{\mathrm{E}}_{\mathrm{m}}/\partial p)_T$ is usually negative. However, if the liquid alkane is at a temperature close to its critical temperature, a large increase in the excess molar enthalpy with pressure occurs. This behavior is illustrated in Figure 15, which gives the $H^{\mathrm{E}}_{\mathrm{m}}(x)$ results at 298.15 K for (ethane + propan-1-ol) (95-ott/lem). (The critical temperature of ethane is 305.50 K.)

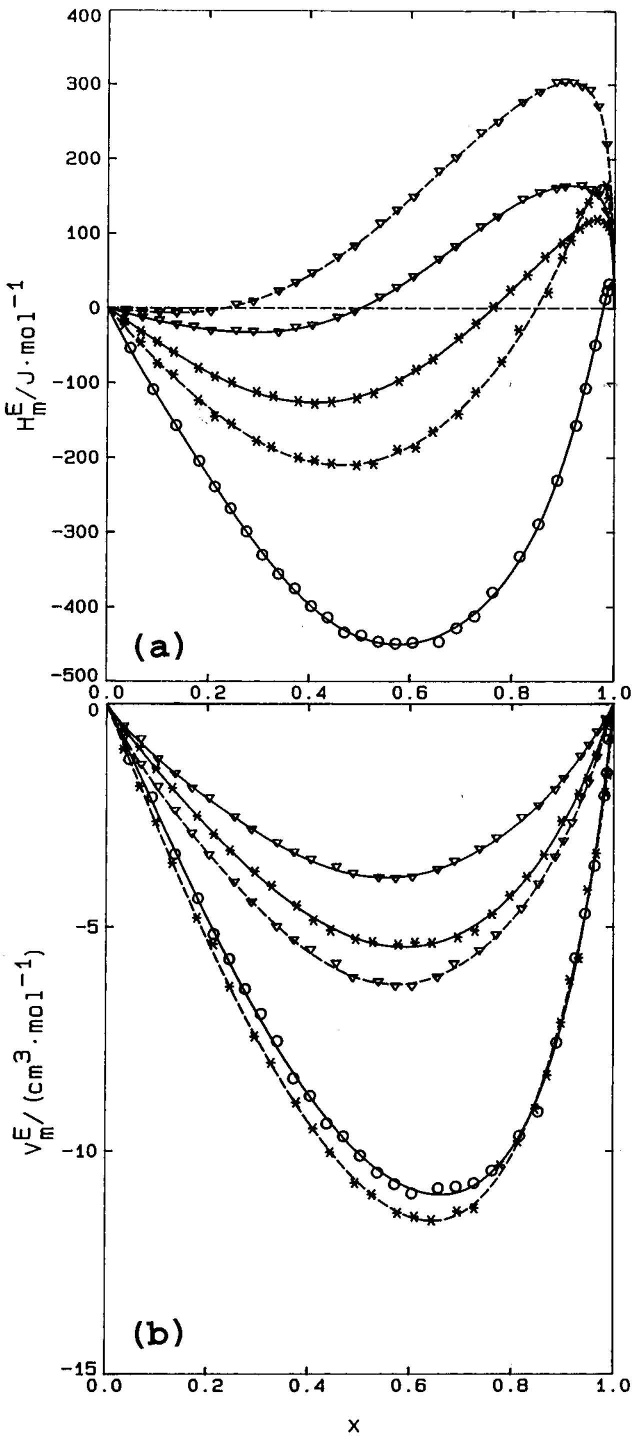

Figure 15. Excess molar enthalpies (a) and excess molar volumes (b) for $\{xC_2H_6 + (1 - x)CH_3(CH_2)_2OH\}$ (95-ott/lem). The solid lines give the results at 298.15 K and the broken lines at 323.15 K. The pressures are (○), 5 MPa; (∗), 10 MPa, (▽), 15 MPa.

Equation 12 relates the pressure coefficient $(\partial H_m^E/\partial p)_T$ to V_m^E. As is evident in Figure 15, $(\partial H_m^E/\partial p)_T$ is large and positive near the critical temperature of the alkane. Under these conditions, V_m^E is negative. Hence, $(\partial V_m^E/\partial T)_p$ must be large and negative to compensate.

Negative values of V_m^E and H_m^E for (alkane + alkanol) mixtures near the critical temperature of the alkane have been explained (90-ott/sip) as due to condensation of the liquid, but "gaslike" alkane into the liquid alkanol. This is similar to the "condensation effect" introduced by Patterson and colleagues (79-des/van).

b. Gas Mixtures. Not many excess molar enthalpy measurements have been reported in the literature for mixtures of gases at high pressures. More measurements would be useful, since data on such mixtures are of special interest in testing equations of state. Interaction virial coefficients can also be calculated from H_m^E for gas mixtures. Results for several investigators have been summarized by Ott and Wormald (94-ott/wor).

Special care is required to obtain reliable H_m^E for gas mixtures, since errors resulting from pressure gradients and Joule–Thomson effects can become important. Ott and Wormald (94-ott/wor) have described these problems in detail and summarized procedures to follow in minimizing the error.

Beenakker and co-workers (65-bee/van) reported measurements of H_m^E for simple gas mixtures containing H_2, N_2, CO, CH_4, and Ar. The measurements were made at near-ambient temperatures and at pressures up to 15 MPa. Other investigators have reported measurements for (N_2 + CO_2) (70-lee/mat, 71-hej/kat), (N_2 + CH_4) (71-kle/ben), (CO_2 + C_2H_4) (79-ba/kal), and (CH_4 + H_2S) (82-bar/kal).

Ott and Wormald (94-ott/wor) have reported that H_m^E for mixtures containing the gases He, Ar, H_2, N_2, CO, CO_2, and CH_4 could be satisfactorily predicted using the Redlich–Kwong and BWR equations of state. Excess molar enthalpies for steam with methane, ethane, propane, or butane were well fitted with the virial equation of state using the virial coefficients B, C, and D for steam (89-wor/lan). The same equation applied to the (steam + n-hexane) and the (steam + n-heptane) systems gave good results only at lower pressures. A special cubic equation was formulated to fit the results at pressures up to 12.6 MPa.

c. Mixtures Containing a Supercritical Fluid. Gruszkiewicz has measured H_m^E for (ethene + ethane) (95-gru/sip) and for (chloromethane + ethane, propane, or butane) (92-gru/sip, 93-gru/ott, 93-gru/ott1) at pressures from (5 to 15) MPa and temperatures from (273.15 to 363.15) K, including some results where both components are liquid, where one is liquid and the other is a supercritical fluid, and where both are supercritical fluids. Measurements near the critical locus are included. The Redlich–Kwong, Soave, and Peng–Robinson equations of state were used to predict H_m^E for these systems (96-gru/ott). A prediction method based upon the principal of corresponding states also worked well on these relatively simple systems (96-gru/ott).

The measurements of Sipowska et al. (91-sip/ott-1) on $\{xC_2H_6 + (1 - x)CH_3(CH_2)_3OH\}$ at the temperatures 298.15, 323.15, and 348.15 K and the pressures 5, 10, and 15 MPa are shown in Figure 16. At 298.15 K, liquid ethane is mixed with liquid butan-1-ol. At the two higher temperatures, the ethane is a supercritical fluid, since T_c = 305.50 K.

A striking feature of Figure 16 is the large pressure effect on H_m^E, especially when the ethane is supercritical, with phase separation occurring at 5 MPa (as evidenced by the linear region of the $H_m^E(x)$ curves), and H_m^E changing from negative to positive as the pressure increases from 10 to 15 MPa, with the change being the largest at the highest temperature.

Ott et al. (89-ott/nee), et. al. have studied in detail the pressure effect on H_m^E for $\{xC_2H_6 + (1 - x)CH_3CN\}$ at temperatures where the ethane is supercritical. The excess molar enthalpy along the isopleth (x = 0.2) at 348.15 K is shown in Figure 17. At a pressure near 5 MPa (which is very nearly the critical pressure of the ethane), H_m^E has a value of approximately −350 J·mol^{-1} and changes only slowly with pressure. At approximately 8 MPa, H_m^E starts to increase rapidly with pressure and levels off at a value of approximately 600 J·mol^{-1} at 15 MPa.

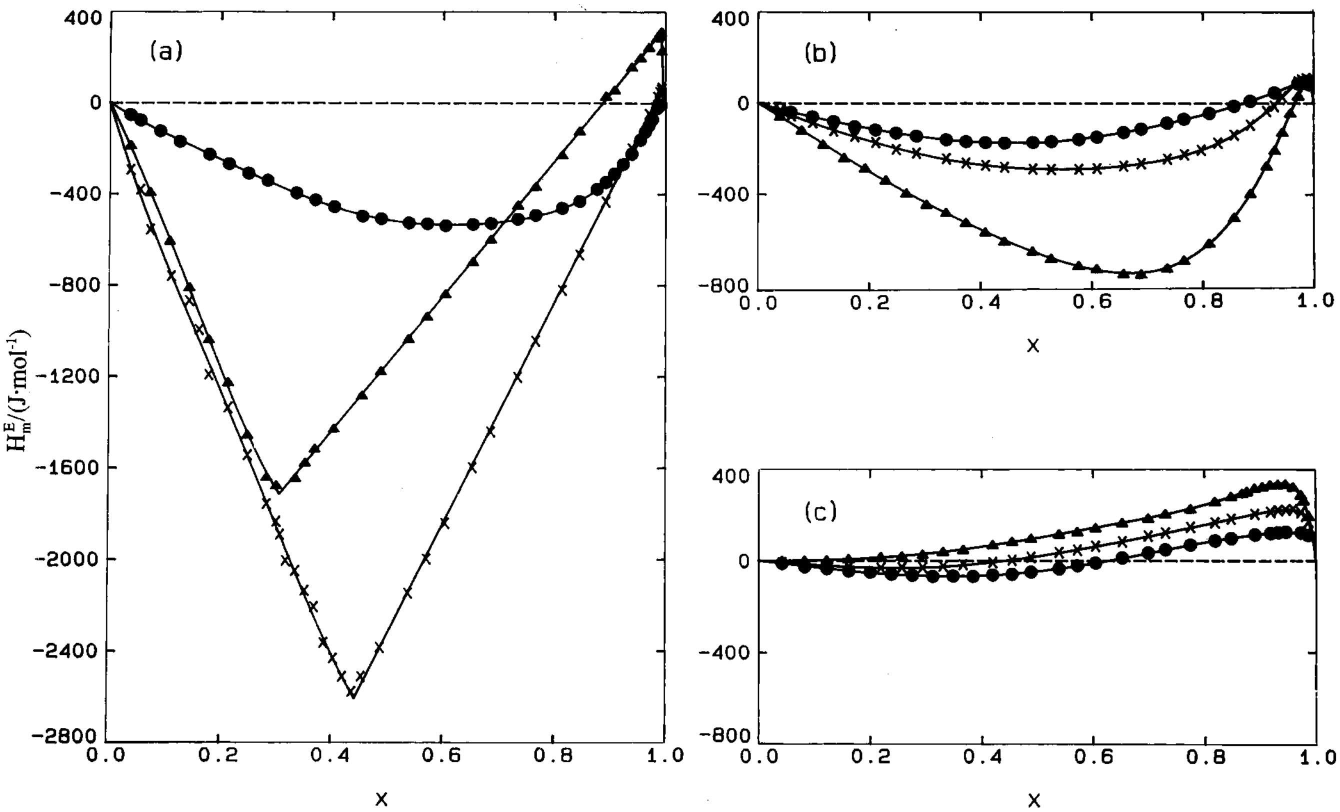

Figure 16. Pressure and temperature effect on the excess molar enthalpies for $\{xC_2H_6 + (1 - x)CH_3(CH_2)_3OH\}$ (91-sip/ott-1) at (a) 5 MPa, (b) 10 MPa, and (c) 15 MPa. The temperatures are as follows: (●) 298.15 K; (×) 323.15 K; (▼) 348.15 K. The ordinate has the same scale for the three graphs so that comparisons of the magnitude of H^E_m can be made at the three pressures. Reprinted with permission from ref 91-sip/ott-1. Copyright 1991 Academic Press.

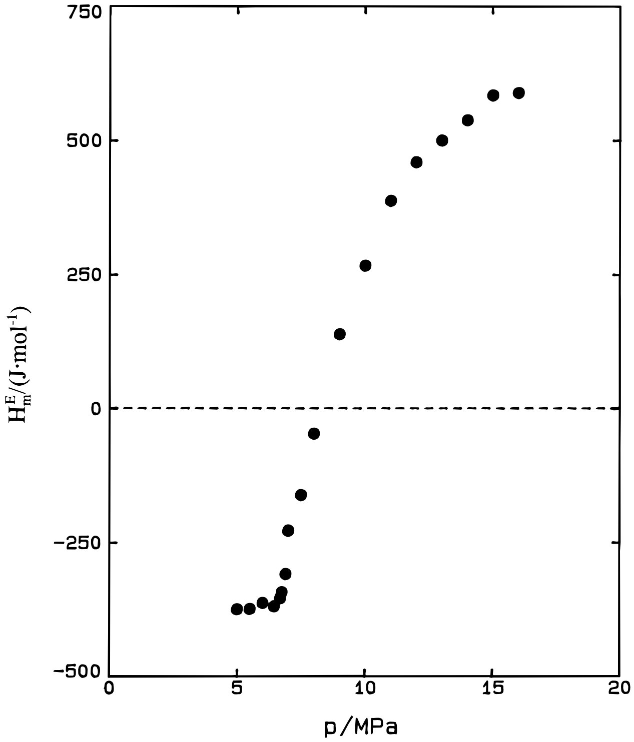

Figure 17. Excess molar enthalpies (89-ott/nee) at 348.15 K for $\{xC_2H_6 + (1 - x)CH_3CN\}$ as a function of pressure along the isopleth $x = 0.2$. Reprinted with kind permission from ref 89-ott/nee. Copyright 1989 Elsevier Science - NL, Sara Burgerhartstraat 25, 1055 KV Amsterdam, The Netherlands.

These effects can be explained by assuming that at the low pressures (near 5 MPa) the ethane is behaving "gaslike." This gas, when it mixes with the liquid acetonitrile, condenses to a liquid and the enthalpy of condensation is released, resulting in a relatively large negative H^E_m. At high pressures (15 MPa and above) the supercritical fluid is compressed to the point that it is behaving "liquidlike" and a positive H^E_m is obtained, which is of the magnitude obtained when a liquid containing polar molecules is mixed with a liquid containing nonpolar molecules. At intermediate pressures (around 10 MPa), the ethane is changing from "gaslike" to "liquidlike" as the pressure increases, and intermediate values for H^E_m are obtained.

Brown and co-workers (96-bro/ott) have recently completed measurements of H^E_m on mixtures of (propane + ethene) at pressures ranging from (5 to 15) MPa and temperatures from (273.15 to 373.15) K, including measurements at the critical temperature of propane (369.82 K). Figure 18 summarizes the effect of pressure on this system at T = (298.15, 323.15, 348.15, 363.15, 369.82, and 373.15) K. These results demonstrate the complexity in H^E_m that can occur, even for simple hydrocarbon mixtures, when measurements are made near the critical locus. A striking feature is the change in H^E_m with temperature at p = 5 MPa. These results have been explained as resulting from a change with temperature of the relative contributions to H^E_m of condensation effects and vaporization effects. These results are in good qualitative agreement with predictions made by Wormald (86-wor) using the van der Waals equation of state.

d. Measurements in the Near-Critical Region. Excess molar enthalpies are very difficult to measure in the near-critical region. The difficulties are caused by large pressure and temperature coefficients $(\partial H^E_m/\partial p)_T$ and $(\partial H^E_m/\partial T)_p$ and large density fluctuations. It has been reported (94-ott/wor) that acceptable H^E_m measurements can be made, although with difficulty, at temperatures

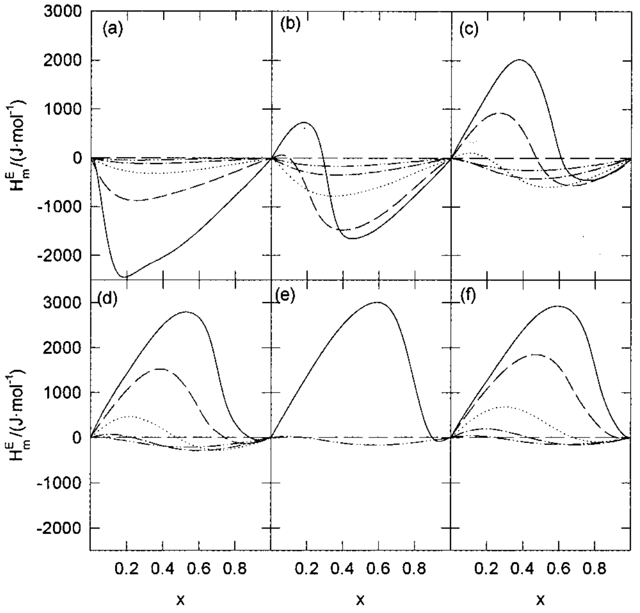

Figure 18. Effect of pressure on the excess enthalpy for $\{xC_3H_8 + (1 - x)C_2H_4\}$ at the temperatures (a) 298.15 K, (b) 323.15 K, (c) 348.15 K, (d) 363.15 K, (e) 369.82 K, and (f) 373.15 K. The lines are representations of the experimental results using fitting equations described in the text. The indications of the various pressures are represented as follows: (—) 6 MPa; (- - -) 7.5 MPa; (···) 10 MPa; (– • –12.5 MPa; (– •• –) 15 MPa. Reprinted with permission from ref 96-bro/ott. Copyright 1996 Academic Press.

within 1 K and pressures within 10 kPa of the critical locus. At temperatures and pressures this close to the critical locus, care must be taken to make sure that the residence time in the calorimeter is sufficient for the components to mix completely, and this condition is not often met in excess molar enthalpy measurements. Measurements closer to the critical locus than the above are generally not successful, even under the most careful conditions.

Figure 19, which shows H_m^E results for (ethane + methanol) at 298.15 K and 5 (96-ott/sip), 6 (96-ott/sip), and 7.5 (89-sip/gra) MPa, demonstrates problems that can occur. The measurements were made at a temperature 7.35 K below T_c for ethane, with the 5 MPa results at a pressure only 90 kPa above p_c for ethane.

It appears from Figure 19 that at 5 and 6 MPa, it is difficult to obtain equilibrium, since scattered results are obtained, but more complicated phase effects may also be occurring. (Ethane + methanol) is a type III system (Scott and van Konynenburg's classification (70-sco/van)), which is distinguished by the absence of a continuous {gas (g) + liquid (l)} critical locus. The curve consists of two branches, one of which ends at an upper critical end point, while the other branch passes through a maximum and a minimum and then increases very rapidly to a very high pressure as the temperature is decreased. At temperatures and pressures just below the upper critical end point, such as T = 298.15 K and p = (5 and 6) MPa for (ethane + methanol), three different two-phase equilibria can be obtained, depending upon the pressure and composition. A $(l_1 + g)$ equilibrium is present at a pressure below a three-phase $(l_1 + l_2 + g)$ surface, with $(l_1 + l_2)$ and $(l_2 + g)$ equilibria possible above the surface. Only small changes in pressure or composition are required to change from one equilibrium to another. With the possibility for large pressure gradients at (p, T) conditions this close to a critical point, it is not unreasonable to separate the H_m^E results shown in Figure 19 into stable and metastable $H_m^E(x)$ curves. What appears to be two different linear regions at p = 5 MPa supports this explanation, since they could result from two different phase equilibria.

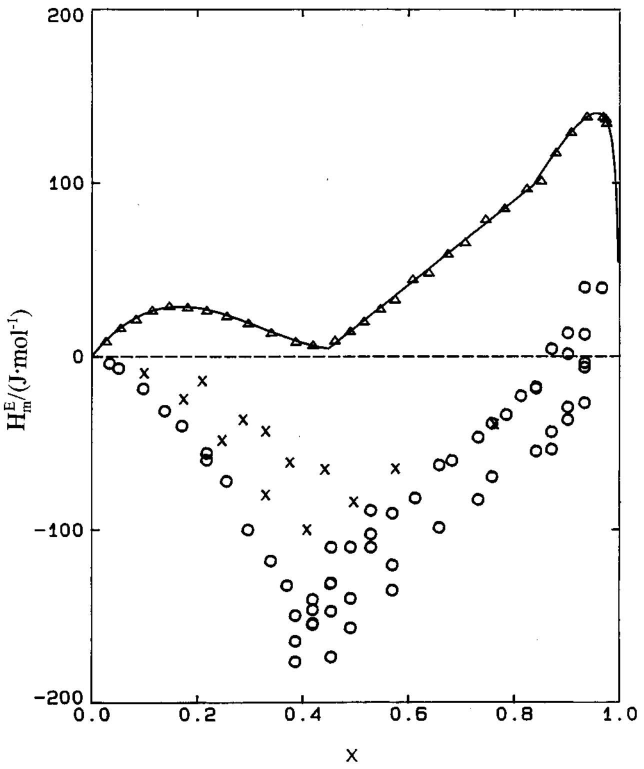

Figure 19. Excess molar enthalpies for $\{xC_2H_6 + (1 - x)CH_3OH\}$ at 298.15 K and the pressures (○) 5.0 MPa; (×), 6.0 MPa, (△) 7.5 MPa (89-sip/gra). The differences in reproducibility of the results at the three pressures are explained in the text.

At a pressure of 7.5 MPa, phase separation is still present, as evidenced by the linear region of the $H_m^E(x)$ curve. However, at this higher pressure, reproducible results are obtained. This pressure aparently is enough higher than the pressure at the upper critical end point so that metastable equilibrium does not occur.

An interesting feature of H_m^E in the near-critical region is its dependence on the relative positions of the critical points of the pure components and the critical locus of the mixture and whether the critical region is approached from the liquid or the gaseous side. For example, H_m^E for (propane + dichlorodifluoromethane) (85-chr/cor) changes from values of -1.75 kJ·mol^{-1} to $+3.1$ kJ·mol^{-1}, depending on the composition and temperatures of the mixture. The large negative values were obtained at a temperature 3.2 K higher than T_c for propane while the large positive values were observed at a temperature 0.5 K lower than T_c for the dichlorodifluoromethane.

6. Applications of Calorimetry to Phase Equilibria Studies

Calorimetric measurements of H_m^E as a function of composition can be used to predict (fluid + fluid) phase equilibria when it occurs. Figure 20 is a graph representing the measured H_m^E in (propane + acetonitrile) at 5 MPa and a series of temperatures (91-ott/sip). (Liquid + liquid) equilibria are present in this system, and the linear regions of the $H_m^E(x)$ curves result when phase separation occurs. These lines represent an average of H_m^E for the two solutions in equilibrium, and hence, do not represent H_m^E for mixing in a single phase.

The compositions corresponding to the intersection of the straight lines with the $H_m^E(x)$ curves (points A and B in

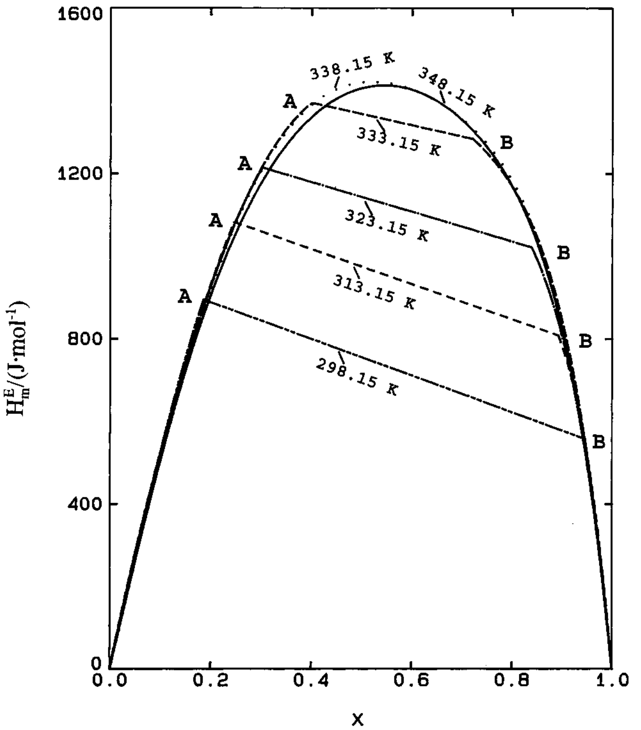

Figure 20. Excess molar enthalpies for $\{xC_3H_8 + (1 - x)CH_3CN\}$ (91-ott/sip) at a pressure of 5 MPa and a series of temperatures. The intersection of the straight lines with the $H^E_m(x)$ curves at points A and B give the compositions of the phases in equilibrium at the various temperatures.

Figure 20) are the solubility limits for the two phases in equilibrium and can be used to construct the (liquid + liquid) phase diagram. Villanañán et al. (84-vil/all) were among the first to apply this method. Ott and colleagues have used the procedure to measure (liquid + liquid) equilibria in several systems (89-ott/nee, 91-ott/sip, 88-ott/pur, 89-sip/gra, 94-gru/ott).

(Vapor + liquid) equilibrium data can also be obtained from $H^E_m(x)$ results. Figure 21, which shows $H^E_m(x)$ curves at several temperatures and a pressure of 5 MPa for (ethane + chloromethane) (93-gru/ott-1), is an example in which (vapor + liquid) equilibrium is present. Again, the linear regions result from phase separation, in this case (vapor + liquid) equilibria. The intersections of the straight lines with the $H^E_m(x)$ curves give the compositions of the liquid and vapor phases in equilibrium.

The $H^E_m(x)$ curves in Figure 21 are typical of what are obtained when a supercritical fluid (such as ethane) dissolves in a liquid (such as chloromethane). At low x, the gaseous ethane dissolves in the liquid chloromethane and H^E_m is negative due to the enthalpy of condensation. At high x, the liquid chloromethane vaporizes into the gaseous ethane and H^E_m is positive, principally due to the enthalpy of vaporization of the liquid chloromethane.

Figure 22 is a three-dimensional (T, p, x) phase diagram for $\{xC_2H_6 + (1 - x)CH_3Cl\}$ (93-gru/ott-1), showing the vapor pressure curves for the pure components and the critical locus. The (T, x) equilibrium values were obtained from the intersection of the $H^E_m(x)$ curves with the straight lines in Figure 21, which were then used to construct the (T, x) constant-pressure phase diagram.

(Liquid + liquid) equilibrium (T, x) points can be accurately obtained from $H^E_m(x)$ results only at temperatures at least (10 to 20) K below the upper critical solution temperature (UCST). At these temperatures, the intersection of the $H^E_m(x)$ curves with the straight lines can be accurately obtained. The procedure could also be applied to systems where a lower critical solution temperature

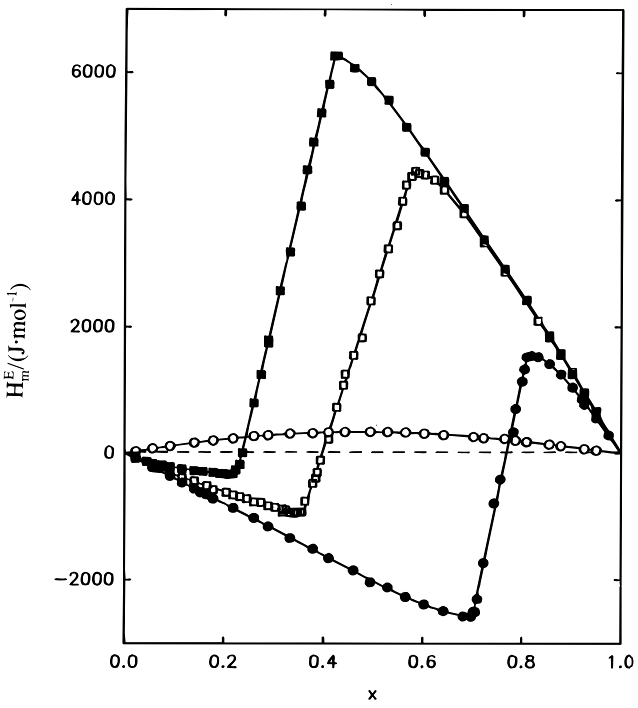

Figure 21. Excess molar enthalpies for $\{xC_2H_6 + (1 - x)CH_3C1\}$ (93-gru/ott) at 5 MPa and the temperatures (○) 298.15 K, (●) 323.15 K, (□) 348.15 K, and (■), 363.15 K. The straight line regions result from (vapor + liquid) equilibrium.

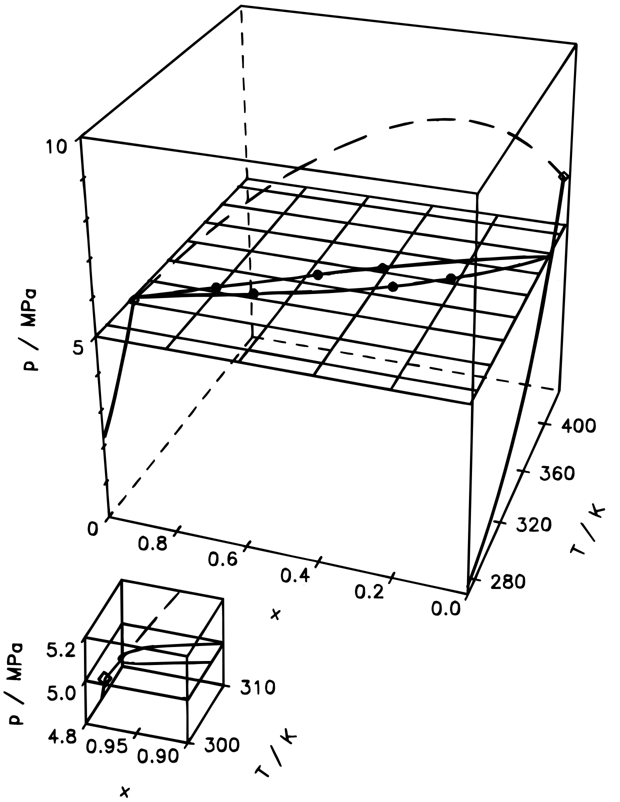

Figure 22. Three-dimensional phase diagram for $\{xC_2H_6 + (1 - x)CH_3Cl\}$ (93-gru/ott-1) at 5 MPa; ● compositions of the vapor and liquid in equilibrium obtained from the H^E_m results shown in Figure 21. The insert in the lower left-hand corner of the figure illustrates that at low x, the $T(x)$ (vapor + liquid) equilibrium isobar intersects the critical locus just above the critical point of ethane. Reprinted with permission from ref 93-gru/ott-1. Copyright 1993 Academic Press.

(LCST) is present. In this case, accurate results would be obtained only at temperatures at least (10 to 20) K above the LCST.

Various procedures have been used to extrapolate the results to the UCST. Ott and colleagues have fitted their results for systems such as (propane + acetonitrile) (91-ott/sip) to the equation

$$T = T_c + k|y - y_c|^{1/\beta} \tag{16}$$

where

$$y = \alpha x/\{1 + x\{\alpha - 1)\} \tag{17}$$

$$y_c = \alpha x_c/\{1 + x_c(\alpha - 1)\} \tag{18}$$

In these equations, T_c and x_c are the critical temperature and critical mole fraction, respectively, and α and k are fitting coefficients. The coefficient β is the critical exponent, which is known to have a value of around 0.32.

By setting β at a value of 0.32 and using equilibrium (T, x) results obtained from $H_m^E(x)$ measurements, one can use eqs 16−18 to predict T_c. The procedure is subject to considerable error since, as discussed earlier, only $H_m^E(x)$ results well below the UCST can be used to obtain reliable equilibrium (T, x) results, and the extrapolation is a long one to the critical point.

Gruszkiewicz et al. (94-gru/ott) have recently described a procedure in which they insert a sapphire capillary in the exit line of a flow calorimeter and use it to visually observe T_c. A combination of this visual measurement of T_c with (T, x) results obtained from $H_m^E(x)$ measurements, (all of which are obtained in the flow calorimeter) can be fitted to eqs 16−18 to obtain reliable (liquid + liquid) (T, x) phase diagrams.

Cordray (87-cor/chr) et al. have described an extrapolation method for obtaining the critical locus from (vapor + liquid) results obtained calorimetrically. They calculate κ at a specified pressure and a series of temperatures, where κ is defined as

$$\kappa = x_g/x_l \tag{19}$$

with x_g and x_l the compositions of the vapor and liquid phases, respectively, as determined from the $H_m^E(x)$ results. They then plot 1n κ vs 1n T and extrapolate to 1nκ = 0 where the resulting T is the critical temperature T_c. The problem with this method is that the extrapolation is not linear and is difficult to do. As a result, the T_c values obtained are not very accurate.

There are advantages and disadvantages to using H_m^E results rather than the more conventional visual methods to determine (fluid + fluid) phase diagrams. The advantages are that H_m^E and equilibrium (T, x) results are obtained over a wide range of temperature and pressure conditions from the same set of measurements and both types of data are often useful in understanding and designing processes such as extraction and other separation schemes, and for theoretical interpretation. The disadvantages are that a large number of H_m^E measurements are required to establish each phase diagram, since each $H_m^E(x)$ curve gives only two equilibrium points. As described earlier, another serious disadvantage is that the method does not work well for measurements near the UCST or LCST, since the linear section of the $H_m^E(x)$ curve becomes short and the end points are difficult to locate precisely. This disadvantage can be largely overcome if the (T, x) results obtained from $H_m^E(x)$ are combined with T_c measurements obtained by visual observation of the effluent from the flow calorimeter as described earlier.

7. Equations for Representing Excess Enthalpy Results

Equation 20, a power series expansion in mole fraction often referred to as the Redlich−Kister equation, is the one most commonly used to express H_m^E results as a function of mole fraction x

$$H_m^E = x(1 - x)\sum_{j=0}^{n} a_j(1 - 2x)^j \tag{20}$$

where the a_j's are fitting coefficients.

Equation 20, with all coefficients equal to zero except for a_0, is parabolic in form with the maximum ($a_0 > 0$) or minimum ($a_0 < 0$) centered at $x = 0.5$. It represents H_m^E results for only the very simplest of systems, and frequently higher order a_j terms are needed to fit the shape of the $H_m^E(x)$ curve. Coefficients with odd values of j compensate for the asymmetry in H_m^E, while coefficients with even values of j narrow or broaden the parabolic shape. Higher order coefficients add bulges (or depressions) to take care of unusual shapes in the $H_m^E(x)$ curves. Care must be taken not to add too many coefficients in an attempt to improve the fit since oscillations may occur which do not correctly represent the experimental results.

A skewing factor k is often added to eq 20 to give

$$H_m^E = x(1 - x)\sum_{j=0}^{n} a_j(1 - 2x)^j/\{1 - k(1 - 2x)\} \tag{21}$$

Care must be taken to restrict k to a value in the range ($-1 < k < 1$) to avoid discontinuities. Equation 21 is used when the maximum or minimum in $H_m^E(x)$ is displaced to high or low x. When this skewing occurs, eq 21 represents the experimental results better and with fewer coefficients than does eq 20, and successfully represents $H_m^E(x)$ results within experimental accuracy for many binary nonelectrolyte mixtures. However, there are still a number of systems that cannot be fitted with either eq 20 or 21 and more complicated expressions are required. Examples of such systems are mixtures containing hydrogen bonds such as (alcohols + hydrocarbons) or (alcohols + water).

Ott, et al. (87-ott/sto) have successfully fitted H_m^E results for (ethanol + water) with

$$H_m^E = x(1 - x)\{S\sum_{j=0}^{n} a_j(1 - 2x)^j + (1 - S)\sum_{k=0}^{m} b_k(1 - 2x)^k\} \tag{22}$$

where a_j and b_k are fitting coefficients and S is given by

$$S = e^{-\alpha x} \tag{23}$$

or

$$S = 1 - e^{-\alpha x} \tag{24}$$

The function S in eqs 23 and 24 can be thought of as a switching function which changes the fit of $H_m^E(x)$ from a power series in ($1 - 2x$) with coefficients that apply at lower values of x to a different power series, again in ($1 - 2x$), with coefficients that apply at higher values of x. With eq 23, the switch occurs at low x, while with eq 24, the switch occurs at high x. In eqs 23 and 24, α is a fitting coefficient that determines the sharpness of the switch.

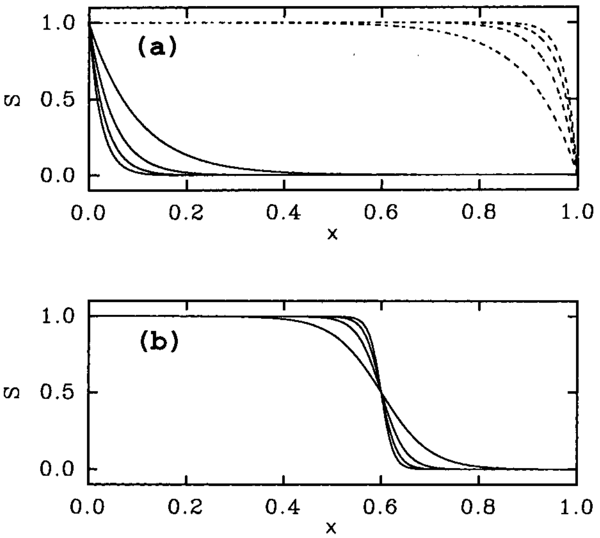

Figure 23. Curves of the switching function S as given by (a) eqs 23 and 24 and (b) eq 25. In (a), the solid line represents eq 23 and the broken line is obtained from eq 24. The values of α used in plotting eqs 23 and 24 are 10, 20, 30, and 40, with the larger value of α corresponding to the steeper curve (sharper switch). In (b), the values of A are 10, 20, 30, and 40, with the larger values of A corresponding to the steeper curve (sharper switch). The value of B was set at 0.6 in eq 25 for all four curves.

Equation 22 combined with eq 23 or 24 works well for systems such as (ethanol + water) where the switch is made at low mole fractions (of alcohol). However, the nature of the switching function is such that it does not work well when the switch is to be made at intermediate mole fractions. Figure 23a is a graph of eqs 23 and 24, illustrating how S changes with mole fraction and parameter α.

Gruszkiewicz et al. (93-gru/ott) have proposed a different switching function, as given in

$$S = 0.5[1 - \tanh\{A(x - B)\}] \tag{25}$$

where A determines the sharpness of the switch and B sets the value of x where the switch occurs. Equation 25 causes the switch to occur at intermediate mole fractions, as shown in Figure 23b. This function has been used in combination with eq 22 to successfully represent $H_{\mathrm{m}}^{\mathrm{E}}(x)$ results for (ethane + chloromethane) (93-gru/ott) at pressures near the critical point of ethane where $H_{\mathrm{m}}^{\mathrm{E}}(x)$ has an unusual shape and appears to have potential for successfully fitting $H_{\mathrm{m}}^{\mathrm{E}}$ results obtained under conditions where unusual dependence on composition is present.

Other investigators (85-chr/cor, 77-mar, 84-chr/wal, 85-chr/zeb, 83-chr/chr) have used rational functions as given by the equation

$$H_{\mathrm{m}}^{\mathrm{E}} = x(1 - x)[\sum_{j=0}^{n} c_j(1 - 2x)^j/\{1 + \sum_{k=0}^{m} d_k(1 - 2x)^k\}] \tag{26}$$

to fit $H_{\mathrm{m}}^{\mathrm{E}}$ results with unusual dependence on x. Equation 26 appears to be about as effective in fitting these $H_{\mathrm{m}}^{\mathrm{E}}(x)$ results as eq 22 with eq 25, but eq 26 has the problem that discontinuities can occur unexpectedly at certain mole fractions. Methods have been developed by King and Queen (79-kin/que) and by Heiser and Parrish (89-hei/par) to help choose parameters which will prevent these discontinuities from occurring. Heiser and Parrish (89-hei/par) have shown benefits in using eq 26 for calculating derivatives of $H_{\mathrm{m}}^{\mathrm{E}}$ with respect to x.

Equations 20−26 are simply empirical fits of $H_{\mathrm{m}}^{\mathrm{E}}(x)$ results and find application in smoothing and summarizing experimental measurements. Other semitheoretical equations such as the Wilson (64-wil), NRTL (68-ren/pra), and UNIQUAC (75-abr/pra) are described in the literature. They were originally developed from equations for calculating $G_{\mathrm{m}}^{\mathrm{E}}$ and activity coefficients with a built-in temperature dependence. The $H_{\mathrm{m}}^{\mathrm{E}}$ forms of these equations are complicated and are usually used only when there is an interest in providing a correlation between $G_{\mathrm{m}}^{\mathrm{E}}$ and $H_{\mathrm{m}}^{\mathrm{E}}$ results. A comparison of the above equations is given in reference 88-chr/row.

In summary, excess molar enthalpy measurements on nonelectrolyte mixtures continues to be a fertile field for further study. The excess molar enthalpy remains an important probe to use in understanding the interactions and structure of liquid mixtures. Of special interest are studies at high pressures and temperatures, especially in the near-critical and supercritical fluid regions. Measurements under these conditions have only begun to come forth in the last few years with the development of flow calorimeters, and much interesting work remains to be done.

Literature Cited

05-cla	Clarke, B. M. Determination of Several Heats of Mixing. *Phys. Z.* **1905**, *5*, 154−159.
07-bos	Bose, E. Calorimetric Studies. *Z. Phys. Chem.* **1907**, *58*, 585−624.
15-bau	Baud, M. E. Thermal Analysis of Binary Mixtures. *Bull. Soc. Chim. Fr.* **1915**, *17*, 329−345.
17-key/hil	Keyes, D. B.; Hildebrand, J. H. Study of the System: Aniline-Hexane. *J. Am. Chem. Soc.* **1917**, *39*, 2126−2137.
25-hir	Hirobe, H. I. Thermochemical Studies. II. The Thermochemistry of Concentrated Solutions. Part 1. *J. Fac. Sci., Imp. Univ. Tokyo.* **1925**, *1*, 155−222.
27-par/caf	Parks, G. S.; Caffee, C. S. Physical Chemical Properties of Mixtures of Acetone and Isopropyl Alcohol. *J. Phys. Chem.* **1927**, *31*, 439−447.
52-bar	Barker, J. A. Coöperative Orientation Effects in Solution. *J. Chem. Phys.* **1952**, *20*, 1526−1532.
55-can/che	Canning, J.; Cheesman, G. H. Heat of Mixing of Liquids. *J. Chem. Soc.* **1955**, *1955*, 1230−1233.
56-bro/foc	Brown, I.; Foch, W. Heats of Mixing. II. Acetonitrile and Nitromethane Systems. *Aust. J. Chem.* **1956**, *9*, 180−183.
58-dri/kiv	Drinkard, W.; Kivelson, D. Nuclear Resonance and Thermal Studies on Hydrogen Bonds in Solution. *J. Phys. Chem.* **1958**, *62*, 1494−1498.
61-lar/mcg	Larkin, J. A.; McGlashan, M. L. The Heat of Mixing. New Calorimeter for Heat of Mixing of Benzene with Carbon Tetrachloride. *J. Chem. Soc.* **1961**, *1961*,3425−3432.
61-mra/van	Mrazek, R. V.; Van Ness, H. C. Heats of Mixing: Alcohol-Aromatic Binary Systems at 25°, 35°, and 45° C. *AIChE J.* **1961**, *7*, 190−195.
62-ott/goa	Ott, J. B.; Goates, J. R.; Budge, A. H. Solid-Liquid Phase Equilibrium and Solid Compound Formation in Mixtures of Aromatic Compounds with Carbon Tetrachloride. *J. Phys. Chem.* **1962**, *66*, 1387−1390.
64-wil	Wilson, G. M. Vapor-Liquid Equilibrium. XI. A New Expression for the Excess Free Energy of Mixing. *J. Am. Chem. Soc.* **1964**, *86*, 127−130.
65-bee/van	Beenakker, J. J. M.; van Eijnsbergen, B.; Knoester, M.; Taconis, K. W.; Zandbergen, P. Heat of Mixing and the Volume Change on Mixing of Gases as a Function of Temperature and Pressure. *Proc. Symp. Thermophys. Prop.* **1965**, *3*, 114−121.
66-qui	Quitzsch, K. Thermodynamics of Binary Liquid Mixtures with Homologous Formamides III. System Carbon Tetrchloride−Dimethylformamide. *Z. Phys. Chem. (Leipzig)* **1966**, *233*, 321−333.

66-sav/win Savini, C. G.; Winterhalter, D. R.; Kovach, L. H.; Van Ness, H. C. Endothermic Heats of Mixing by Isothermal Dilution Calorimetry. *J. Chem. Eng. Data* **1966**, *11*, 40–43.

66-vil/sta Vilcu, R.; Stanciu, F. Excess Thermodynamic Functions from Calorimetric Data. *Rev. Roumaine Chim.* **1966**, *11*, 175–182.

66-win/van Winterhalter, D. R.; Van Ness, H. C. An Isothermal Dilution Calorimeter for Exothermic Heats of Mixing. *J. Chem. Eng. Data* **1966**, *11*, 189–192.

67-ras/nat Rastogi, R. P.; Nath, J.; Misra, J. Thermodynamics of Weak Interactions in Liquid Mixtures. I. Mixtures of Carbon Tetrachloride, Benzene, Toluene, and p-Xylene. *J. Phys. Chem.* **1967**, *71*, 1277–1286.

68-ren/pra Renon, H.; Prausnitz, J. M. Local Compositions in Thermodynamic Excess Functions for Liquid Mixing. *AIChE J.* **1968**, *14*, 135–144.

69-bro/foc Brown, I.; Fock, W.; Smith, F. The Thermodynamic Properties of Solutions of Normal and Branched Alcohols in Benzene and n-Hexane. *J. Chem. Thermodyn.* **1969**, *1*, 273–291.

69-mar/sto Marsh, K. N.; Stokes, R. H. Enthalpies of Mixing of n-Hexane + Cyclohexane at 25 °C. *J. Chem. Thermodyn.* **1969**, *1*, 223–225.

69-sto/mar Stokes, R. H.; Marsh, K. N.; Tomlins, R. P. An Isothermal Displacement Calorimeter for Endothermic Enthalpies of Mixing. *J. Chem. Thermodyn.* **1969**, *1*, 211–221.

69-sto/mar-1 Stokes, R. H.; Marsh, K. N.; Tomlins, R. P. Enthalpies of Exothermic Mixing Measured by the Isothermal Displacement Calorimeter for Cyclo-octane + Cyclopentane at 25 °C. *J. Chem. Thermodyn.* **1969**, *1*, 377–379.

70-ewi/lev Ewing, M. B.; Levien, B. J.; Marsh, K. N.; Stokes, R. H. Excess Enthalpies, Excess Volumes, and Excess Gibbs Free Energies for Mixtures of Cyclooctane + Cyclopentane at 288.15, and 308.15 K. *J. Chem. Thermodyn.* **1970,** *2*, 689–695.

70-ewi/mar Ewing, M. B.; Marsh, K. N. Enthalpies of Mixing of Cyclohexane + Carbon Tetrachloride, of Cyclohexane + Cyclopentane, and of Carbon Tetrachloride + Cyclopentane at Various Temperatures. *J. Chem. Thermodyn.* **1970**, *2*, 351–358.

70-ewi/mar-1 Ewing, M. B.; Marsh, R. H.; Tuxford, C. W. The Isothermal Displacement Calorimeter: Design Refinements. *J. Chem. Thermodyn.* **1970**, *2*, 751–756.

70-lee/mat Lee, J. I.; Mather, A. E. The Excess Enthalpy of Gaseous Mixtures of Nitrogen and Carbon Dioxide. *J Chem. Thermodyn.* **1970**, *2*, 881–895.

70-nak/tou Nakanishi, K.; Touhara, H.; Watanabe, N. Associated Solutions II. Heat of Mixing of Methanol with Aliphatic Amines. *Bull. Chem. Soc. Jpn.* **1970**, *43*, 2671–2676.

70-sco/van Scott, R. L.; Van Konynenburg, P. H. Static Properties of Solutions. van der Waals and Related Models for Hydrocarbon Mixtures. *Discuss. Faraday Soc.* **1970**, *49*, 87–97.

71-ben/mur Benson, G. C.; Murakami, S.; Jones, D. E. G. The Thermodynamic Properties of Acetone + Cyclohexanol Mixtures at 25 °C. *J. Chem. Thermodyn.* **1971**, *3*, 719–731.

71-cle/pig Clever, H. L.; Pigott, S. P. Enthalpies of Mixing of Dimethylsulfoxide with Water and with Several Ketones at 298.15 K. *J. Chem. Thermodyn.* **1971**, *3*, 221–225.

71-hej/kat Hejmadi, A. V.; Katz, D. L.; Powers, J. E. Experimental Determination of the Enthalpy of Mixing of N_2 + CO_2 Under Pressure. *J. Chem. Thermodyn.* **1971**, *3*, 483–496.

71-kle/ben Klein, R. R.; Bennett, C. O.; Dodge, B. F. Experimental Heats of Mixing for Gaseous Nitrogen and Methane. *AIChE J.* **1971**, *17*, 958–965.

71-sli Slifkin, M. A. *Charge Transfer Interactions of Biomolecules*; Academic Press: London, 1971; p 25.

72-cam/ana Campbell, A. N.; Anand, S. C. Phase Equilibriums in the Systems Acetone-Methanol, Acetone-Cyclohexane, Methanol-Cyclohexane, and Acetone-Methanol-Cyclohexane. *Can. J. Chem.* **1972**, *50*, 479–489.

74-ewi/mar Ewing, M. B.; Marsh, K. N. Excess Functions for Cyclopentane + Cyclohexane, Cyclopentane + Cycloheptane, and Cyclohexane + Cyclo-octane. *J. Chem. Thermodyn.* **1974**, *6*, 395–406.

74-ewi/mar-1 Ewing, M. B.; Marsh, K. N.; Excess Functions forCyclohexane + Cycloheptane and Cycloheptane + Cyclo-octane. *J. Chem. Thermodyn.* **1974**, *6*, 1087–1096.

74-kiy/ana Kiyohara, O.; Anand, S. C.; Benson, G. C. The Thermodynamic Properties of Acetone + Cyclopentanol Mixtures at 298.15 K. *J. Chem. Thermodyn.* **1974**, *6*, 355–360.

74-pic Picker, P. New Concepts in Design and Applications of Flow Microcalorimetry. *Can. Res. Dev.* **1974**, Jan-Feb, 11–16.

75-abr/pra Abrams, D. S.; Prausnitz, J. M. Statistical Thermodynamics of Liquid Mixtures: A New Expression for Excess Gibbs Energy of Partly or Completely Miscible Systems. *AIChE J.* **1975**, *21*, 116–128.

75-han/fen Handa, Y. P.; Fenby, D. V. Calorimetric Study of the Deuterium Isotope Effects in Liquid Mixtures. *J. Chim. Phys. Phys.-Chim. Biol.* **1975**, *72*, 1235–1240.

76-bel Bellemans, A. Statistical Thermodynamics of Dilute Solutions of Alcohols and Alkanes. *Rocz. Chem.* **1976**, *50*, 1749–1754.

76-chr/han Christensen, J. J.; Hansen, L. D.; Eatough, D. J.; Izatt, R. M.; Hart, R. M. Isothermal High Pressure Flow Calorimeter. *Rev. Sci. Instrum.* **1976**, *47*, 730–734.

76-ell/wor Elliott, K.; Wormald, C. J. A Precision Differential Flow Calorimeter. The Excess Enthalpy of Benzene + Cyclohexane between 280.15 K and 393.15 K. *J. Chem. Thermodyn.* **1976**, *8*, 881–893.

77-ewi/mar Ewing, M. B.; Marsh, K. N. Thermodynamics of Cycloalkane + Cycloalkane Mixtures: Comparison with Theory. *J. Chem. Thermodyn.* **1977**, *9*, 863–871.

77-mar Marsh, K. N. A General Method for Calculating the Excess Gibbs Free Energy from Isothermal Vapour-Liquid Equilibria. *J. Chem. Thermodyn.* **1977**, *9*, 719–724.

77-sto Stokes, R. H. Interpretation of the Thermodynamic, Spectroscopic and Dielectric Properties of Solutions of Ethanol in Cyclohexane in Terms of Association. *J. Chem. Soc., Faraday Trans. 1.* **1977**, *73*, 1140–1148.

77-wor/lew Wormald, C. J.; Lewis, K. L.; Mosedale, S. The Excess Enthalpies of Hydrogen + Methane, Hydrogen + Nitrogen, Methane + Nitrogen, Methane + Argon, and Nitrogen + Argon at 298 and 201 K at Pressures up to 10.2 MPa. *J. Chem. Thermodyn.* **1977**, *9*, 27–42.

78-mar Marsh, K. N. The Measurement of Thermodynamic Excess Functions of Binary Liquid Mixtures. In *Chemical Thermodynamics, Vol. 2;* McGlashan, M. L., Ed.; *The Chemical Society:* Burlington House: London, 1978; p 38.

79-ba/kal Ba, L. B.; Kaliaguine, S. C.; Ramalho, R. S. Excess Enthalpies of Binary Gaseous System Ethylene + Carbon Dioxide by Flow Calorimetry. *Can. J. Chem. Eng.* **1979**, *57*, 363–366.

79-des/van De St.-Romain, P.; Van, H. T.; Patterson, D. Effects of Molecular Flexibility and Shape on the Excess Enthalpies and Heat Capacities of Alkane Systems. *J. Chem. Soc., Faraday Trans. 1* **1979**, *75*, 1700–1707.

79-fre/ric French, H. T.; Richards, A.; Stokes, R. H. Thermodynamics of the Partially Miscible System Ethanol+Hexadecane. *J. Chem. Thermodyn.* **1979**, *11*, 671–686.

79-kin/que King, M. B.; Queen. N. M. Use of Rational Functions for Representing Data. *J. Chem. Eng. Data* **1979**, *24*, 178–181.

79-wóy Wóycicka, M. K. Excess Enthalpies of Dilute Solutions of 3-Ethyl-3-Pentanol in n-Heptane. *Bull. Acad. Pol. Sci., Ser. Sci. Chim.* **1979**, *27*, 331–334.

80-cos/hod Costigan, M. J.; Hodges, L. J.; Marsh, K. N.; Stokes, R. H.; Tuxford, C. W. The Isothermal Displacement Calorimeter: Design Modifications for Measuring

Exothermic Enthalpies of Mixing. *Aust. J. Chem.* **1980**, *33*, 2103−2119.

80-hei/lic Heintz, A.; Lichtenthaler, R. N. Excess Enthalpies of Liquid Alkane Mixtures at Pressures up to 500 Bar. I. Experimental Results. *Ber. Bunsen-Ges. Phys. Chem.* **1980**, *84*, 727−732.

80-mar/ott Marsh, K. N.; Ott, J. B.; Costigan, M. J. Excess Enthalpies, Excess Volumes, and Excess Gibbs Free Energies for (n-Hexane + n-Decane) at 298.15 and 308.15 K. *J. Chem. Thermodyn.* **1980**, *12*, 343−348.

80-ott/mar Ott, J. B.; Marsh, K. N.; Stokes, R. H. Excess Enthalpies, Excess Gibbs Free Energies, and Excess Volumes for (Cyclohexane + n-Hexane), and Excess Gibbs Free Energies and Excess Volumes for (Cyclohexane + Methylcyclohexane) at 298.15 and 308.15 K. *J. Chem. Thermodyn.* **1980**, *12*, 1139−1148.

80-val/lop Valero, J.; Lopez, M. C.; Garcia, M.; Gutiérrez Losa, C. Excess Enthalpies of Some (Bromoalkane + Alkane) Mixtures. *J. Chem. Thermodyn.* **1980**, *12*, 627−633.

81-hei Heintz, A. The Pressure Dependence of the Excess Enthalpies of Mixtures of Isopropanol with Heptane and Isooctane up to 553 Bar. *Ber. Bunsen-Ges. Phys. Chem.* **1981**, *85*, 632−635.

81-nag/tam Nagata, I.; Tamura, K.; Tokuriki, S. Excess Enthalpies and Complex Formation of Acetonitrile with Acetone, Chloroform, and Benzene. *Thermochim. Acta* **1981**, *47*, 315−331.

82-bar/kal Barry, A. O.; Kaliaguine, S. C.; Ranalho, R. S. Excess Enthalpies of the Binary System Methane-Hydrogen Sulfide by Flow Calorimetry. *J. Chem Eng. Data* **1982**, *27*, 436−439.

82-chr/han Christensen, J. J.; Hanks, R. W.; Izatt, R. M. *Handbook of Heats of Mixing;* John Wiley and Sons: New York, 1982.

83-chr/chr Christensen, J. J.; Christensen, S. P.; Schofield, R. S.; Faux, P. W.; Harding, P. R.; Izatt. R. M. The Excess Enthalpies of (Carbon Dioxide + Cyclohexane) at 308.15, 358.15, and 413.15 K from 7.50 to 12.50 MPa. *J. Chem. Thermodyn.* **1983**, *15*, 1151−1157.

84-bus/hol Busey, R. H.; Holmes, H. F.; Mesmer, R. E. The Enthalpy of Dilution of Aqueous Sodium Chloride to 673 K Using a New Heat-Flow and Liquid-Flow Microcalorimeter. Excess Thermodynamic Properties and Their Pressure Coefficients. *J. Chem. Thermodyn.* **1984**, *16*, 343−372.

84-chr/gme Christensen, C.; Gmehling, J.; Rasmussen, P.; Weidlich, U. Heats of Mixing Data Collection; Part 1, Binary Systems and Part 2, Binary and Multicomponent Systems. In *Vol. III of Chemistry Data Series;* Behrens, P., Eckermann, R., Eds.; DECHEMA: Frankfurt, 1984.

84-chr/iza Christensen, J. J.; Izatt, R. M. An Isothermal Flow Calorimeter Designed for High Temperature, High Pressure Operation. *Thermochim. Acta* **1984**, *73*, 117−129.

84-chr/wal Christensen, J. J.; Walker, T. A. C.; Schofield, R. S.; Faux, P. W.; Harding, P. R.; Izatt, R. M. The Excess Enthalpies of (Carbon Dioxide + Hexane) at 308.15, 358.15, and 413.15 K from 7.50 to 12.50 MPa. *J. Chem. Thermodyn.* **1984**, *16*, 445−451.

84-vil/all Villamañán, M. A.; Allawl, A. J.; Van Ness, H. C. Vapor/Liquid Equilibrium and Heats of Mixing for Diethyl Ether/Water at 35 °C. *J. Chem. Eng. Data.* **1984**, *29*, 431−435.

85-bat/row Battler, J. R.; Rowley, R. L. Excess Enthalpies Between 293 and 323 K for Constituent Binaries of Ternary Mixtures Exhibiting Partial Miscibility. *J. Chem. Thermodyn.* **1985**, *17*, 719−732.

85-chr/cor Christensen, J. J.; Cordray, D. R.; Zebolsky, D. M.; Izatt, R. M. The Excess Enthalpies of (Propane + Dichlorodifluoromethane) from 353.15 to 398.15 K at 4.45 MPa. *J. Chem. Thermodyn.* **1985**, *17*, 335−348.

85-chr/zeb Christensen, J. J.; Zebolsky, D. M.; Izatt, R. M. The Excess Enthalpies of (Carbon Dioxide + Toluene) at 470.15 and 573.15 K from 7.60 to 12.67 MPa. *J. Chem. Thermodyn.* **1985,** *17*, 1−10.

86-ott/sto Ott, J. B.; Stouffer, C. E.; Cornett, G. V.; Woodfield, B. F.; Wirthlin, R. C.; Christensen, J. J.; Deiters, U. K. Excess Enthalpies for (Ethanol + Water) at 298.15 K and Pressures of 0.4, 5, 10 and 15 MPa. *J. Chem. Thermodyn.* **1986**, *18*, 1−12.

86-wor Wormald, C. J. Heats and Volumes of Mixing in the Critical Region. An Exploration Using the van der Waals Equation. *Fluid Phase Equilib.* **1986**, *28*, 137−152.

87-cor/chr Cordray, D. R.; Christensen, J. J.; Izatt, R. M. A Calorimetric Method for the Determination of Binary Phase Compositions at High Temperatures and Pressures. *Sep. Sci. Technol.* **1987**, *22*, 1169−1181.

87-ott/sto Ott, J. B.; Stouffer, C. E.; Cornett, G. V.; Woodfield, B. F.; Che, G.; Christensen, J. J. Excess Enthalpies for (Ethanol + Water) at 398.15, 423.15, 448.15, and 473.15 K and at Pressures of 5 and 15 MPa. Recommendations for Choosing (Ethanol + Water) as an H^{E}_{m} Reference Mixture. *J. Chem. Thermodyn.* **1987**, *19*, 337−348.

88-chr/row Christensen, J. J.; Rowley, R. L.; Izatt, R. M. *Handbook of Heats of Mixing. Supplementary Volume*; John Wiley and Sons: New York, 1988.

88-ott/pur Ott, J. B.; Purdy, J. E.; Neely, B. J.; Harris, R. A. Excess Enthalpies at 323.15, 348.15, and 373.15 K, and (Liquid + Liquid) Equilibria for (Cyclohexane + Acetonitrile) at 0.4 and 15 MPa. *J. Chem. Thermodyn.* **1988**, *20*, 1079−1087.

89-fun/wet Funke, H.; Wetzel, M.; Heintz, A. New Applications of the ERAS Model. Thermodynamics of Amine + Alkane and Alcohol + Amine Mixtures. *Pure Appl. Chem.* **1989**, *61*, 1429−1439.

89-hei/par Heiser, R. F.; Parrish, W. R. Representing Physical Data With Rational Functions. *Ind. Eng. Chem. Res.* **1989**, *28*, 484−489.

89-ott/nee Ott, J. B.; Neely, B. J.; Purdy, J. E.; Owen, R. L. Excess Enthalpies for Ethane + Acetonitrile at 298.15, 323.15, and 348.15 K and at 7.5 and 15 MPa. *Thermochim. Acta* **1989**, *154*, 71−79.

89-sip/gra Sipowska, J. T.; Graham, R. C.; Neeley, B. J.; Ott, J. B.; Izatt, R. M. Excess Enthalpies for (Ethane + Methanol) at 298.15 and 348.15 K and 7.5 and 15 MPa, and at 323.15 K at 7.5, 10, and 15 MPa. *J. Chem. Thermodyn.* **1989**, *21*, 1085−1093.

89-wor/lan Wormald, C. J.; Lancaster, N. M. A Cubic Equation of State for Mixtures Containing Steam. *J. Chem. Soc., Faraday Trans.1* **1989**, *85*, 1315−1326.

90-ott Ott, J. B. Calorimetry and Phase Equilibria: A Marriage Made in Heaven. *J. Chem. Thermodyn.* **1990**, *22*, 1129−1151.

90-ott/sip Ott, J. B.; Sipowska, J. T.; Owen, R. L.; Izatt, R. M. Excess Enthalpies for (Ethane + Ethanol) at (298.15, 323.15, and 348.15) K and at (5, 10, and 15) MPa. *J. Chem. Thermodyn.* **1990**, *22*, 683−694.

91-ott/sip Ott, J. B.; Sipowska, J. T.; Izatt, R. M. Excess Enthalpies for (Propane + Acetonitrile) at the Temperatures (298.15, 313.15, 323.15, 333.15, 338.15, and 348.15) K and at the Pressures (5, 10, and 15) MPa. Determination of (Liquid + Liquid) Equilibria from the Calorimetric Results. *J. Chem. Thermodyn.* **1991**, *23*, 687−698.

91-sip/ott Sipowska, J. T.; Ott, J. B.; Neely, B. J.; Izatt, R. M. Excess Enthalpies for (Propane + Methanol) at the Temperatures (298.15, 323.15, 348.15, and 373.15) K and Pressures (5, 10, and 15) MPa, and at 363.15 K and (5 and 15) MPa. *J. Chem. Thermodyn.* **1991**, *23*, 551−559.

91-sip/ott-1 Sipowska, J. T.; Ott, J. B.; Woolley, A. T.; Izatt, R. M. Excess Enthalpies for (Ethane + Butan-1-ol) at (298.15, 323.15, and 348.15) K and at (5, 10, and 15) MPa. *J. Chem. Thermodyn.* **1991**, *23*, 1013−1021.

92-gru/sip Gruszkiewicz, M. S.; Sipowska, J. T.; Ott, J. B.; Graham, R. C. Excess Enthalpies for (Butane + Chloromethane) at the Temperatures (298.15, 323.15, and 348.15) K and pressures (5 and 15) MPa and at the Temperature 293.15 K and Pressure 15 MPa. *J. Chem. Thermodyn.* **1992**, *24*, 1057−1064.

92-woo/sip Woolley, A. T.; Sipowska, J. T.; Ott, J. B.; Izatt, R. M. Excess Enthalpies for (Butane + Acetonitrile) at the Temperatures (298.15, 323.15, and 348.15) K and at the Pressures (5, 10, and 15) MPa. *J. Chem. Thermodyn.* **1992**, *24*, 965−971.

93-gru/ott Gruszkiewicz, M. S.; Ott, J. B.; Sipowska, J. T. Excess Enthalpies for (Propane + Chloromethane) at the Temperatures (298.15, 323.15, and 348.15) K and Pressures (5 and 15) MPa and at the Temperature 363.15 K and Pressures (5, 10, and 15) MPa. *J. Chem. Thermodyn.* **1993**, *25*, 385−390.

93-gru/ott-1 Gruszkiewicz, M. S.; Ott, J. B.; Sipowska, J. T. Excess Enthalpies for (Ethane + Chloromethane) at the Temperatures (298.15, 323.15, 348.15, and 363.15) K and Pressures from 5 MPa to 16 MPa. *J. Chem. Thermodyn.* **1993,** *25*, 1017−1029.

94-gru/ott Gruszkiewicz, M. S.; Ott, J. B.; Sipowska, J. T. An Apparatus for Measuring the Upper Critical Solution Temperature Using the Effluent from a Flow Calorimeter: Application to Mixtures of Acetonitrile with Cyclohexane, Propane, and Butane. *Thermochim. Acta* **1994**, *245*, 155−161.

94-let/dom Letcher, T. M.; Domańska, U. The Excess Molar Enthalpies of (Acetonitrile + an Ether) at the Temperature 298.15 K. *J. Chem. Thermodyn.* **1994**, *26*, 113−119.

94-ott/wor Ott, J. B.; Wormald, C. J. Excess Enthalpy by Flow Calorimetry. In *Experimental Thermodynamics Vol. IV-Solution Thermodynamics;* Marsh, K. N., O'Hare, P. A. G., Eds.; Blackwell Scientific Publishers: London, 1994; Chapter 8, pp 161−194.

95-gru/sip Gruszkiewicz, M. S.; Sipowska, J. T.; Ott, J. B.; Brown, P. R. Excess Enthalpies for (Ethane + Ethene) at the Temperatures (273.15, 298.15, 323.15, 348.15, and 363.15) K and the Pressures (5, 7.5, 10, 12.5, and 15) MPa. *J. Chem. Thermodyn.* **1995**, *27*, 507−524.

95-ott/lem Ott, J. B.; Lemon, L. R.; Sipowska, J. T.; Brown, P. R. Excess Enthalpies and Excess Volumes for (Ethane + Propan-1-ol) at the Temperatures (298.15, 323.15, and 348.15) K and at the pressures (5, 10, and 15) MPa. *J. Chem. Thermodyn.* **1995**, *27*, 1033−1045.

96-bro/ott Brown, P. R.; Ott, J. B.; Lemon, L. R.; Moore, J. D. Excess Enthalpies for (Propane + Ethene) Over the Temperature Range from 273.15 K to 373.15 K and the Pressure Range from 4 MPa to 15 MPa. *J. Chem. Thermodyn.*, in press.

96-gru/ott Gruskiewicz, M. S.; Ott, J. B. Excess Enthalpies of (Ethane + Ethene), (Ethane + Chloromethane), (Propane + Chlormomethane), and (Butane + Chloromethane) from Cubic Equations of State and the Principle of Corresponding States--A Comparison with Experimental Data. *Fluid Phase Equilib.*, in press.

96-ott/bro Ott, J. B.; Brown, P. R.; Sipowska, J. T. Comparison of Excess Molar Enthalpies and Excess Molar Volumes as a Function of Temperature and Pressure for Mixtures of (Ethane, Propane, and Butane) With (Methanol, Ethanol, Propan-1-ol, and Butan-1-ol). *J. Chem. Thermodyn.* **1996**, *28*, 379−404.

96-ott/goa Ott, J. B.; Goates, J. R. Summary of Melting and Transition Temperatures of Pure Substances and Congruent and Incongruent Melting Temperatures of Molecular Addition Compounds. *J. Chem. Eng. Data* **1996**, *41*, 669−677.

96-ott/sip Ott, J. B.; Sipowska, J. T. Unpublished H_m^E results for $\{xC_2H_6 + (1 - x)CH_3OH\}$ at a Temperature of 298.15 K and Pressures of 5 and 6 MPa.

Received for review March 18, 1996. Accepted June 5, 1996.⊗

JE960105A

⊗ Abstract published in *Advance ACS Abstracts,* July 15, 1996.